8-2014

A Novel Cell Based Assay for MMP Inhibitor Screening

Pantrika Krisanarungson
University of Arkansas, Fayetteville

A Novel Cell Based Assay for MMP Inhibitor Screening

A Novel Cell Based Assay for MMP Inhibitor Screening

A thesis in partial fulfillment
of the requirements for the degree of
Master of Science in Biomedical Engineering

By

Pantrika Krisanarungson
Chulalongkorn University
Bachelor of Engineering, 2010

August 2014
University of Arkansas

This thesis is approved for recommendation to the graduate council

_____
Dr. Jeffrey C. Wolchok
Thesis Director

_____
Dr. Matt McIntosh
Committee Member

_____
Dr. David Zaharoff
Committee Member

ABSTRACT

Up to date, a plethora of protein based materials are used as implants to stimulate tissue regeneration or fillers to alleviate tissue or organ impairment. This includes glottal insufficiency, urinary bladder incontinence and especially in cosmetic industrial to improve facial contour. Once in vivo, protein-based materials are decomposed by cell secreted matrix metalloproteinases (MMP) and lose their volume within months [1, 2, 3, 4]. By introducing MMP inhibitor (MMPI), the extent of material degradation over time may be reduced. In this dissertation, the development of cell-based assay capable of identifying MMPI candidates for protein-based implant lifetime prolongation is described. To visualize the degradation, DQ-gelatin, (heavily fluorescence labeled gelatin that emits fluorescence signal proportional to its degradation) was used to represent the implant material. This gelatin was co-cultured with NIH-3T3 in a 96-well plate supplemented with growth media under standard tissue culture condition (5% CO_2, 95% humidity at 37°C). Number of seeded cells, DQ-gelatin concentration and experiment run time were varied to optimize signal-to-noise ratio whilst taking into account more than 80% of seeded cells must remain viable. With optimized parameters, 0.8 million cells cultured on cell adhesion support scaffold in presence of 50 µg/mL DQ-gelatin for 5 days, the efficacy of BB-94 and TIMP-1 as synthetic and natural MMPI candidate were investigated. Both BB-94 and TIMP-1 were tested at different concentrations according to their IC_{50} and the approximated amount of MMPs in tissue fluid, 20-1000 nM and 0.1-2 µg/mL respectively, to determine their most efficient dosage. BB-94 and TIMP-1 demonstrated maximum potential at 72.59±4.75 % and 60.00±27.41 % at the concentration of 1000 nM and 2 µg/mL respectively. Statistical Analysis could not detect the significant difference from varying MMP inhibitor concentration, therefore, their concluded most efficient dosage in our experiment is the lowest concentration used for

testing. Because our assay generated reliable statistically distinct signals and are capable of detecting quantitative inhibitory efficacy of MMP inhibitors, we believe our novel cell-based assay is a feasible method for MMP inhibitor screening that could better represent the complex degradation process of protein-based implants in biological systems than the current conventional enzyme-based methods.

ACKNOWLEDGMENTS

Firstly, I would like to express my gratitude to my adviser Dr. Jeffrey Collins Wolchok for granting me opportunity to gain research experience, submitting scientific abstract and presenting at well regarded conference. I am very thankful for the research assistantship position and for being able to earn MS degree in Biomedical Engineering. Secondly, I would like to show my appreciations to my thesis committees Dr. Matt McIntosh, Dr. David Zaharoff and other professors including Dr. Jin, Dr. Tian, Dr. Rhoads, Dr. Sakon, Dr. Mauromoustakos, Dr. Li, Dr. Erf, Dr. Loewer and Dr. Costello for giving me valuable knowledge, advice and research skills. The road would have been a lot more difficult if I had not received their help and guidance. I am very thankful for the knowledge I have obtained made my progress towards graduation.

I wish to acknowledge my fellow student, Addison Walker, for the time and effort he spent on prepare valuable data on cell adhesion support scaffold analysis included in this thesis. All assistance provided is greatly appreciated. Special thanks to my colleagues Bhanu Koppolu, Sean Smith, Lirong Yang, Sruthi Ravindranathan, Jonathan Earls, Andrew Zhou and Hulusi Turgut for all the technical training I have received. I also would like to extend my gratitude to my lab mates, Zahrah Al-Rumaih, Benjamin Kasukonis, Joseph Wyatt and Klaire Wilson for all their supports. Lastly, I would like to offer my sincere gratitude to the most important people, my parents and friends for their encouragement throughout the difficult times. I also would like to extend my appreciation to all those people whom have made my life during the time that I have spent to obtain my master degree wonderful and memorable.

TABLE OF CONTENTS

Chapter 1 Introduction 1

Chapter 2 Literature Review 4

1. Introduction 4

2. Implantable Biomaterial 6

3. Mechanism of Degradation 9

4. Conventional Method and the Comparison to Our Developed Prototype 14

5. Experimental Design and Rationale 19

    5.1. Overview 19

    5.2. DQ-Gelatin 20

    5.3. Cell Type 21

    5.4. Cell Adhesion Support Scaffold 22

    5.5. MMP Inhibitor Timp-1 and BB-94 24

    5.6. Cell Viability Testing 26

6. Experiment Settings 38

7. Conclusion 29

Hypothesis 30

Approach 30

TABLE OF CONTENTS (CONTINUED)

Chapter 3 Novel Assay Development 31

1. Rationale 31

2. Methodology 33

2.1. Cell Adhesion Support Scaffold Preparation 33

2.2. Cell Culture and Propagation of NIH-3T3 34

2.3. Signal Optimization 34

2.3.1. Setting A) 35

2.3.2. Setting B) 35

2.4. NIH-3T3 Viability Testing 36

2.5. Mathematical Model Construction and Statistical Analysis 36

3. Result and Discussion 38

3.1. Setting A) 38

3.2. Setting B) 52

3.3. Overall Result and Discussion 58

4. Conclusion 61

Chapter 4 Cell-Based MMP Inhibitor Screening Assay 63

1. Rationale 63

TABLE OF CONTENTS (CONTINUED)

2. Methodology 64

2.1. Assay Preparation 64

2.2. MMP Inhibitor Screening Assay 64

2.3. NIH-3T3 Viability Testing 65

2.4. Statistical Analyses 66

3. Result and Discussion 66

3.1. MMP Screening Assay 70

4. Conclusion 71

Chapter 5 Conclusion and Future Directions 72

Chapter 6 References 75

CHAPTER 1: INTRODUCTION

At present, there are numerous protein-based materials applications [1, 5-11], both in research developmental stage and in clinical use. Many are utilized for regenerative purposes such as for tissue growth stimulation in cardiac muscle, nerve and cartilage, while some are used as fillers to alleviate glottal insufficiency, urinary incontinence and even in while cosmetic industry to reduce wrinkles. These materials doubtlessly create a lot of impact in our society; however, in most cases, their lifetimes are only a few months after they are implanted. Therefore, it would be very beneficial to be able to prolong their retention time in vivo. In this way, the healing efficacy of the implant is improved, the duration that the implant provides satisfactory effects would be extended and patients would not have to go through the surgical process as often, consequently, improving the community living standard.

Once inside the body, protein based materials are degraded the same way as extracellular matrix (ECM) turnover [12], which is by enzymatic digestion. These specific groups of enzymes are generally referred to as matrix metalloproteinases (MMPs) [13]. They are secreted by both residential cells and infiltrated cells recruited during inflammation after wounds through laceration, injection or damage of tissue has taken place. By inhibiting MMP activities, the retention time of protein-based implants in vivo could be extended. For this reason, our research group is interested in identifying suitable MMP inhibitors (MMPis) and has developed a novel cell based assay for MMPi screening that can analyze the inhibitory effectiveness of each inhibitor.

MMPs are zinc dependent enzymes; all enzymes of this family share a specific structural motif, which is zinc binding domain [14, 15]. By introducing agents capable of forming a complex with MMPs at this structure, the proteolytic activity of MMPs may be inhibited. These agents are referred to as MMP inhibitors. There exist many types of MMPi in nature, the major endogenous inhibitors in tissue are the tissue inhibitors of metalloproteinases (TIMPs) [16]. Due to MMP up-regulation during tumor invasion, a large variety of MMP inhibitors has been synthesized as anticancer drugs. They are effective and relatively inexpensive when compare to natural MMP inhibitors [14].

The current technique most associated with the studies of MMP and their inhibitors is zymography [17]. Zymography or substrate zymography is an electrophoretic method that has been extensively used to study ECM degrading enzymes. It visualizes proteolytic activity based on substrate digestion [18]. Zymography does not give accurate quantification of enzymatic activity [19] nor does it resembles enzymatic degradation in nature. In this research, we construct a cell-based assay prototype capable of screening MMP inhibitors. It provides quantitative data on degradation inhibition efficacy together with the effect of the inhibitor on cell viability. By focusing on cellular modulated degradation, the information obtained should resemble more of the material breakdown after implantation. For substances intended to be used in vivo, they are generally introduced into cell culture to evaluate the substance effect on cell apoptosis after their efficacy testing. Our method reduces the procedure and gives information on both aspects in one assay.

In this thesis, we divide our report into 4 chapters, beginning with chapter 1: introduction to give an overview of our research. Chapter 2: Literature review provides background information on our assay development and the logic behind assay assembly. After the fundamental knowledge has been laid down we describe the method and the outcome of our assay development in Chapter3: Prototype development. In Chapter 4: Cell-based MMP inhibitor screening assay, the result from prototype development were used to assemble our assay and used to examine MMP inhibitor efficacy in impeding protein breakdown.

For simplicity, readers whom are only interested in the developed assay may over look chapter 3 and begin at Cell-based MMP inhibitor screening assay, Chapter 4, as the methodology, result and discussion is complete within its own chapter. Readers may only need to refer to chapter 3 for some repeated methods that has already been described in assay development process. Lastly, the future direction of this research is briefly discussed, Chapter 4.

The findings from our research would provide an alternative method for MMP inhibitor efficacy evaluation and screening to the conventional zymography technique. By proving the possibility of slowing down the degradation of protein-based material using MMP inhibitor, it is highly probable that protein-based implant lifetime prolongation may take place and contribute positive impact to both medical and scientific community.

CHAPTER 2: LITERATURE REVIEW

1. Introduction

In this research we develop a cell based assay prototype for screening potential drugs that may slow degradation of the protein based materials. For better understanding of our assay, the literature review presents the background knowledge necessary for understanding our prototype development. The sections within this chapter include:

1. Introduction
2. Implantable biomaterials
3. Mechanism of degradation
4. Conventional method and the comparison to our developed prototype
5. Experiment design and rationale
    5.1. Overview
    5.2. DQ-gelatin
    5.3. Cell type
    5.4. Selected MMP inhibitor: TIMP-1 and BB-94
    5.5. Cell adhesion support scaffold
    5.6. Cell viability testing
6. Experiment setting
7. Conclusion

We first we describe protein-based materials and their retention time in vivo, **section 1**. Because of the benefit in their lifetime prolongation, our research group looks into the mechanism of biomaterial degradation, **section 2**, to design our assay based on the events that take place in vivo after implantation. After that, we introduce the conventional technique used to study MMP

proteolytic activity, **section 3**, then compare with our developed prototype. In Experiment design and rationale, **section 4**, we describe a rough picture of our prototype, its each component and the logic behind the design. Finally, we summarize our research; how each component is combined to form our assay, outlining our hypothesis and approach, **section 5**.

2. Implantable Biomaterials

When minor laceration occurs, a wound healing mechanism is activated and a proper repair of the laceration take place. But once considerable injury where natural regeneration is not sufficient happens, biomedical associated technology is required to aid the restoration process. Because human regenerative capacity is limited, wrinkles form, organs start to malfunction as people age, scarring and loss of tissue function takes place after severe trauma. To heal these impairments myriads of biomimetic materials are specifically tailored to provide proper 3-dimentional micro-environment and stimulants for cell migration, proliferation, differentiation and cell organization to form new tissue at the wounded site [20-22]. The materials are also engineered to be biocompatible, facilitates transport of nutrients and metabolic waste while having similar mechanical properties to its surroundings, and be able to be remodeled and replaced at a simultaneous rate with neo-tissue formation. These materials have been intensively researched since before 2003 [23].

While biomimetic implants are utilized in many types of tissue repair including bone [5], cartilage [6], nerve [7] and cardiac muscle [8], some are used as space filling agents in the cases of glottal insufficiency [9, 10], urinary bladder incontinence [11] and for rhytide alleviation in cosmetic field [1]. These materials are called fillers after their function. Others are utilized in wound healing stimulations. Because materials with low immunogenicity that hold similar mechanical property to its surrounding tissue are generally natural, they are degraded overtime after implant making their satisfactory effect are not permanent.

Fillers and injectables such as autologous fat have been known since 1893 [24]. It initially was a very appealing as it posts no immunological threats, is easy to harvest with numerous accessible donor sites and remains for over one year [25]. But due to the large volume loss, its popularity has steeply declined. Hyaluronic acid (HA) is one valuable implantable material. They are secreted interstitial molecules by variety of cells lineage to maintain tissue viscosity and shock absorbance [26] and are crucial in joints and voice production, rendering them preferable for vocal fold augmentation [27-31]. Despite their benefits of viscoelastic property, zero immunogenicity [32], wound healing stimulation [33] and well established safety and efficacy profile [34], HA's major drawback is its short-lived nature. Although crosslinking has been performed in attempt to lengthen its lifetime, HA could only be maintained for only 12 weeks [35]. In its natural state, hyaluronic acids have been reported to last less than 2 days subcutaneous [36] and 3-5 days inside vocal fold [37].

Extracellular matrixes (ECM) are cell-secreted mixture of interwoven fibrous proteins and glycosaminoglycans [38-40], containing small amount of cytokines and growth factors that modulates cell behavior [41]. They play a major role in wound healing [42] by stimulating angiogenesis, host cells recruitment, adhesion, proliferation, and remodeling of damaged tissue [43]. ECM based material can recapitulate natural conditions in vivo [44]. Numerous publications have confirmed ECM potential in tissue reconstruction [41] including skin, tissue, vessel, tendon and lower urinary tract. Consequently, ECM represent nature's scaffold for tissue repair although their ability to establish complete restoration may be in question since ECM are rapidly degraded after implant [2, 3].

Collagen is the most abundant protein in the ECM as well as in human body [45, 46]. It is a natural constituent of connective tissue and the primary structural protein of all our organs [47]. Other than providing mechanical support and acting as a reservoir of hormones and growth factor, it plays pivotal role in wound healing process [48]. As implantable material, collagen is the single substance filler most intensively used and has been manufactured in USA since 1977. It has received FDA approval and has become the gold standard used to compare engineered materials for soft tissue augmentation of later generations [49]. Over the years, various collagen based injectables have been developed and commercialized with different compositions and wide-range of residential time in vivo [1, 50-52]. None the less, like other natural materials, all forms of collagen correction are temporary and require periodic maintenance [1, 4].

In short, because of the advantages of implantable protein based materials, both in regeneration stimulation and as volume fillers for treatment, they are utilized in a wide range of applications and cause large impact on biomedical industry. Regrettably, the main drawbacks of protein based implants are their short lived nature; thus lifetime prolongation of these materials would be a vital next step to enhancing therapeutic effects of biomimetic materials.

3. Mechanism of Degradation

By being able to prolong protein based implant lifetime, their therapeutic efficacy would increase, providing many benefits in both the society and the scientific community. For tissue regenerative implants such as ECM-based materials, their stimulatory effect of would be extended, granting better tissue restoration outcome. For filler type materials, its volume may be retained for longer period, thus, widening gaps between each treatment for people who suffer glottal insufficiency, urinary bladder incontinence or requiring cosmetic surgery. Therefore, patients would be provided with more comforts and may lessen their treatment cost in the long run.

To prolong the lifetime of the implant, it is imperative to acknowledge the mechanism of material break down. In general, there are 2 different ways that materials are degraded in vivo; by hydrolysis and enzymatic digestion [53]. The decomposition of polymer-based implant is largely governed by hydrolysis [54], which could easily be controlled by adjusting their chemical composition [55]. Our main focus lies on the degradation of protein based materials, where the decomposition rate cannot be straightforwardly predicted.

Unlike those of polymer-based, the residence time in vivo of protein-based implant is predominated by their host response they elicit. As protein decomposition is tightly regulated by cell secreted proteases and is concentrated at cell periphery [56], the higher the material immunogenicity, the larger cell number are recruited to the implant site, the more concentrated

the secreted protease per area. If the implant is susceptible to cellular infiltration and is prone to enzymatic attack [12] its retention time in vivo is difficult to be prolonged.

From tissue regeneration point of view, the implant site is similar to an injury with subcutaneously embedded foreign body under the skin lesion. The act of incision is enough to trigger wound healing, a specific biological process comprise of 5 overlapping independent stages to reestablish the integrity of the damage tissue [57, 58]. The progression through hemostasis, inflammation, proliferation and remodeling stages make up the wound healing sequence [59-61].

Normal healing response take place as soon as tissue is injured [62]. For instance, during a surgery where bleeding takes place, hemostasis is activated and blood clot forms, sending out chemotactic cues to recruit inflammatory cells such as monocytes and neutrophils to the implant cite for pathogen elimination purposes [63]. The immunogenicity determines the extent of inflammation. Because the degradation is brought about by both resident and infiltrated cells [12], the material porosity influences its degradation rate. Other than surrogating for pathogens, neutrophils and macrophages also functions similar to platelets in fibrin clot signaling for fibroblast and endothelial cells [64]. They gather at the periwound area, infiltrate the clot, proliferate, undergo angiogenesis, lay down extracellular matrix and form new tissue [65]. The newly synthesized tissue or the scar tissue is not as strong as the original. The strength of scar tissue is approximately only 25% of a normal tissue. After several months its mechanical property can be improved by collagen fibers reorganization and cross linking by the fibroblast but it will never regain to its native strength. [66]

The removal of exogenous implants is similar to the regular process of extracellular matrix (ECM) remodeling [12]. Various types of enzymes are secreted by cells within the immediate proximity and digest their specific substrates [67]. The well-known ones are the matrix metalloproteinases (MMPs) for their involvement with wound healing and normal tissue regulation [13]. They are grouped according to their substrates and are critical to the repair processes for eliminating necrotic tissue, fibrin clot that forms after bleeding and are also necessary in cell migration during inflammatory phase [68]. Table 1 summarizes MMPs, their specific substrates and cellular sources [12, 68].

Protein-based implants can be degraded by a diversity of proteases. To mimic the main composition of mammalian tissue [69, 70], many of those implants contain collagen. Fibrillar collagens function to provide mechanical strength and protect the cells they surround, therefore, it is not easily degraded and is resistant to most enzymatic attacks. Collagenase (MMP-1, 8 and 13) are the specific MMPs with the ability to cleave collagen in their triple helical domain. After the cleavage, collagen denature into gelatin at physiological temperature and is susceptible to further digestion by numerous enzymes (MMP-1-3, 7-12, 14, 16-19) including gelatinases (MMP-2 and 9) [71], making it the easier step in matrix (granulation tissue) remodeling [72]. After it is reduced to amino acid, it can be resorbed and re-utilized in cellular protein synthesis.

Because degradation of implant is modulated by cell secreted MMPs, we believe that by inhibiting the activity of MMPs, the implant lifetime could be prolonged. Our objective is to develop an assay that can detect and evaluate substances capable of inhibiting MMP's

proteolytic activity. These substances are referred to as the MMP inhibitors (MMPis). Our developed assay is a cell-based assay to resemble the phenomena of protein-based implant degradation in vivo and to investigate the effect of MMPi on cell viability.

Table 1 Matrix metalloproteinase and their substrate

Enzymes	Substrates
Collagenases	
Collagenase-1 (MMP-1)	Collagen I, II, III, VII, VIII, X, gelatin, aggrecan, versican, proteoglycan link protein, L-selectin, entactin, tenascin, serpins, α2- macroglobulin, TNF precursor, MBP, IGFBP-3
Collagenase-2 (MMP-8)	Collagen I, II, III, VII, VIII, X, gelatin, aggrecan, fibronectin, laminin, serpins, α2-macroglobulin
Collagenase-3 (MMP-13)	Collagen I, II, III (II>I or III), IV, IX, X, XIV, gelatin, aggrecan, perlecan, fibronectin, laminin, tenascin, fibrillin, SPARC, serpins, PAI
Gelatinases	
Gelatinase A, 72 kDa (MMP-2)	Gelatin, collagen I, IV, V, VII, X, XI, XIV, aggrecan, versican, proteoglycan link protein, fibronectin, laminin, laminin-5, tenascin, fibrillin, SPARC, elastin, vitronectin, α2-macroglobulin, TNF precursor, MBP, IGFBP-3
Gelatinase B, 92 kDa (MMP-9)	Gelatin, collagen IV, V, VII, X, XIV, aggrecan, versican, nidogen, proteoglycan link protein, fibronectin, fibrillin, SPARC, entactin,elastin, vitronectin, α1-antitrypsin, α2-macroglobulin, TNF precursor,MBP, angiostatin
Stromelysins	
Stromelysin-1 (MMP-3)	Collagen III, IV, V, IX, X, gelatin, versican, nidogen, aggrecan, perlecan,proteoglycan link protein, fibronectin, laminin, tenascin, fibrillin, SPARC, entactin, elastin, TNF precursor, MBP, IGFBP-3
Stromelysin-2 (MMP-10)	Collagen III, IV, V, gelatin, nidogen, aggrecan, proteoglycan link protein, fibronectin, elastin
Stromelysin-3 (MMP-11)	α1-proteinase inhibitor; weak activity on aggrecan, fibronectin, laminin
Matrilysin (MMP-7)	Collagen IV, gelatin, versican, nidogen, aggrecan, fibronectin, laminin, tenascin, SPARC, elastin, vitronectin, MBP,angiostatin
Metalloelastase (MMP-12)	Collagen IV, gelatin, nidogen, aggrecan, fibronectin, laminin, fibrillin, elastin, vitronectin, α1-antitrypsin, TNF precursor, angiostatin
Membrane-type MMPs	
MT1-MMP (MMP-14)	Collagen I, II, III, gelatin, nidogen, aggrecan, perlecan, fibronectin, laminin, tenascin, vitronectin, fibrillin
MT2-MMP (MMP-15)	Aggrecan, perlecan, fibronectin, laminin, nidogen, tenascin
MT3-MMP (MMP-16)	gelatin, casein
MT4-MMP (MMP-17)	gelatin, TNF precursor
MT5-MMP (MMP-24)	Not determined

Other MMPs	
MMP-18, MMP-19	Gelatin
Enamelysin (MMP-20)	Amelogenin
MMP- 21, 22, 23	Not determined

***Modified from Vaalamo et al.

By providing information regarding their potency in decreased protein decomposition rate and whether they may influence cell apoptosis, we believe implant lifetime prolongation is a very possible advancement in medical and biomaterial field that may eventually propel the society towards a better living standard.

4. Conventional Method and the Comparison to Our Developed Prototype

Zymography or substrate zymography is a technique extensively used for studying ECM degrading enzymes [17], MMPs, the group of enzymes responsible for implant degradation during wound remodeling phase. Zymography is a simple, sensitive, quantifiable and efficient approach for proteolytic activity analysis of cell and tissue extracts [19, 73]. It is preferred over other techniques such as gene expression measurement or immunoassay as most MMPs are encoded as inactive precursors, zymogens, and those assay are not capable of differentiating between the active form and inactive form. Zymogens are subject to multiple post-translational regulations before they become activated in the intercellular space [74, 75].

Zymography was first developed by Gross and Lapière for detecting collagen degradation in 1962. The current widely used "substrate zymography" is the adaptation introduced by Heussen and Dowdle in 1980 [76]. Because MMPs are overexpressed during tumor invasion, this technique has gained large recognition in cancer and other research field around the world and has become a well-accepted conventional method for measuring MMP expression [77]. Zymography has been used in both research and clinical settings. It has been used to discover [78] and identify new types of enzymes [79] or overexpression of enzymes in multiple forms of cancer [80-83] and neurological diseases [84], study enzyme inhibitors [85] and identify their optimal dosage. Zymography is also the key technique for studying proteinases expression and post-translational modifications regulation [86].

Zymography visualizes enzymatic activity on the basis of substrate conversion. It is an electrophoretic method where proteins, particularly enzymes, are separated by size in a reducing SDS gel co-polymerized with protein substrate of choice. SDS inside the gel causes protein to denature into its unfolded state, rendering them to be separated without bias of their three dimensional shape. Upon removal of SDS, the proteins renature and exert proteolytic activity on the protein gel substrate [18]. The enzyme digestion could be viewed by common protein staining technique, Coomassie blue staining. After destaining to remove excess dyes, the proteolytic area will appear as white bands blue background of protein gel substrate. Within a certain linear range, the intensity of the band can be used to quantify the amount of protein associate with its activity. [17, 18]

Over the past 50 years, more than 20 variants of zymography have emerged to improve specific aspects according to different research objectives [88]. The most relevant zymography assays that may be applied to our research are the substrate zymography, reverse zymography (RZ), and in situ zymography (ISZ). The latter 2 variants go by similar concept to substrate zymography. Reverse zymography is used for identification of natural inhibitors such as TIMP which also is a protein. Both Enzyme and substrate are copolymerized within the gel, after staining process, the area containing effective inhibitors is recognize as dark bands containing intact substrate against light background [77, 89].

Although RZ shows the inhibitor potency, it does not provide any information related to cellular response to the inhibitor. The closest method to defining the actual MMP activity in viable tissue

would be in situ zymography. The sample is prepared as a thin section and is brought into contact with the fluorescence substrate. After incubation, the localization of particular proteolytic activity towards the substrate from enzyme within the biological slice sample can be viewed. Identification of the responsible enzymes is carried out by IHC after staining [73, 77, 90]. ISZ is generally used for to pinpoint enzymatic activity but the enzymatic activity can also be estimated. This format of zymography is the only variant that gives the net activity of the enzymes within the sample, not the measure of potential enzymatic activity.

Firstly, quantitation of zymograms remains difficult [19]. The sensitivity of substrate zymography is largely governed by the staining and destaining process. Overstaining of protein dyes causes bands with low activity to become invisible against blue zymogram background. Because estimation of MMPs from sample amount is based on multipoint calibration by dissolving and diluting standards of different enzymes with known concentration, excessive destaining may bleach out bands with high activity, negating the differences between light bands, lowering the sensitivity of enzyme quantification.

Secondly, the MMP activity demonstrated by zymography may not represent their proteolytic capacity in nature. Most MMPs are secreted in their inactive form, zymogens. They are tightly regulated and gain proteolytic activity only after specific enzymatic cleavage [91, 92]. During SDS-gelelectrophoresis in zymography, zymogens are unfolded and its inhibitory peptide is no longer attached from the catalytic site. After SDS removal, the proteins only partially refold resulting in active enzymes instead of the naturally inactive zymogens. Furthermore, the activity

of MMPs is governed by various inhibitors [93] such as tissue inhibitor of matrixmettalloproteinase (TIMP) which inhibits MMPs even if the enzymes are in there active forms. In general, MMP in solution non-covalently forms a complex with their corresponding TIMP. These complexes dissociate in the presence of SDS [94]. Therefore, electrophoresis step creates artifacts of increasing enzymatic activity and zymography may not display the actual proteolytic activity but rather, their possible potential in substrate digestion.

Considering the practicality of MMP inhibitor screening assay, it would useful if the optimal dosage of each inhibitor could be determined. Because electrophoresis unavoidably increases enzymatic activity from that of the natural state [86, 95, 96], substrate zymography may not be the best option. In situ zymography offers advantage over the conventional substrate zymogrphy in the sense that it somewhat provide insights on the net enzymatic activity in living system. But both in situ and in gel zymography are time consuming and a large number of experiments needs to be conducted for testing out different MMP inhibitors and dosages are not suitable for large scale screenings.

We believe the prototype introduced in this study provides a better alternative for screening MMP inhibitors capable of prolonging implant lifetime to other conventional methods. As cells are a living units that response to external stimuli, disruption in ECM remodeling could up-regulate MMP expression and leading to excessive ECM degradation. Results from cell-based assays may simulate degradation of material overtime after implant better than ISZ tissue slice conducted over short time period [66] or common assay with single or multiple enzyme

component where no response from viable components are involved. Adopting 96-well plate setting, our assay can provide comparative efficacy of different inhibitors at different concentrations in couple to their effect on cell viability. In this way, it is possible to visualize optimal dosage with minimal assay runs. Because MMP and their natural inhibitors are relatively expensive, our assay may even prove to be the more efficient method for inhibitor screening.

5. Experimental Design and Rationale

5.1. Overview

Our aim is to assemble an assay prototype for screening potential inhibitors capable of slowing down implants degradation. Because the breakdown of implants takes place in a similar manner as ECM digestion, modulated by MMP catalyzed hydrolysis, our prototype is designed to test out the enzyme inhibitors efficacy while ensuring considerable cell apoptosis is not induced. As the first step towards in vivo testing, this assay is designed and resembles the physiological phenomena that take place around the implant while remain practical and easy to use. Cells are cultured in the presence of fluorescence labelled substrate that emits signals proportional to the extent of its degradation. The inhibitor of choice is added to the culture in a varied amount. The experiment is constructed to give the inhibition efficacy in terms of percentage of the fluorescence intensity given out by the control where MMP inhibitor is not introduced into the cell culture vessel. The distinctive of the signal from background, signal-to-noise ratio, from this assay is optimized by varying number of seeded cells, substrate concentration, reaction time and experiment setting, having or not having cell adhesion scaffold. Cell viability assay is conducted after experiments to estimate how many cells still remain alive after the assay run time.

In this chapter, we describe the rationale behind the assay design; the fluorescence substrate, cell type selection, MMP inhibitor, and the detail of experiment planning and signal optimization in a separate section below.

5.2. DQ-Gelatin

In our assay, a fluorescent signal is used as our means of degradation detection. Cells are cultured in presence of the material representing natural implants, DQ-gelatin. DQ-gelatin is a commercially available gelatin heavily labelled with Fluorescein isothiocyanate (FITC) that emits fluorescence proportional to its own extent of degradation.

In general, the occurrence of fluorescence takes place through relaxation of fluorophores from excited states to its original ground state emitting photons light signals [97]. In DQ-gelatin, the gelatin conjugated FITC are located in such close proximity that one molecule interferes with fluorescence of another, resulting in fluorescence quenching when DQ-gelatin is in its intact state. Once cleaved by gelatinolytic activity, the distance between those fluorophores increases, enabling fluorescence to take place after the conjugated FITC are excited, giving fluorescence emission against weakly fluorescence background [73].

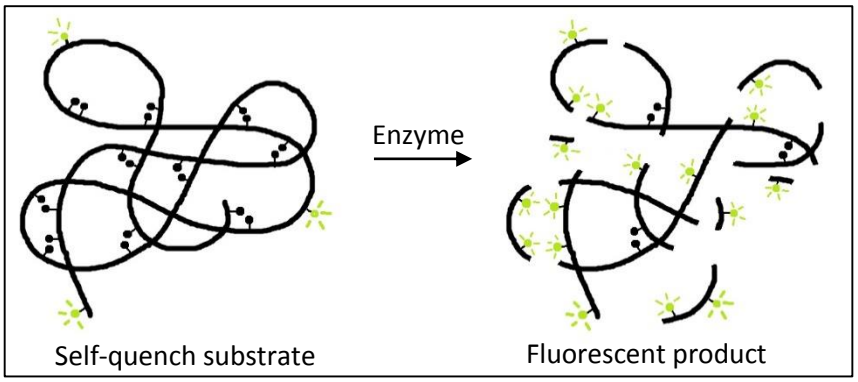

Figure 1 Fluorescence emission in DQ-gelatin. Fluorophores in close proximity interferes with fluorescence activity of one another. Once cleaved, self-quenching effect is dwindled resulting in fluorescence emission upon excitation of the fluorophores.

DQ-gelatin has been used in various MMP related research where cells are cultured in its presence over a prolonged period [98, 99]. From those studies, many studies apply DQ-gelatin in solution form, many as cell substrate such as for in situ zymography to locate proteolytic activity or to measure the efficacy of the enzymes or in some cases, both. From these experiments we assume that DQ-gelatin displays low-toxicity towards living cells in culture. The dye quench DQ-gelatin provides a higher sensitivity than normal fluorescence conjugation and also serves as a good substrate since gelatin can be digested by not only gelatinases but by a large repertoire of enzymes (Table1). Concisely, this commercialized product is selected to portray protein based implants for its similarity to natural gelatin, adequate biocompatibility, as a substrate specific to many groups of MMP and high sensitivity in signal generation proportional to gelatinolytic activity.

5.3. Cell Type

During cellular infiltration of implant in the inflammatory phase, immune cells are recruited to the wounded site along with fibroblast. The Macrophages and neutrophils clears out pathogen, their number increases depending on the implants immunogenicity while fibroblasts migrate to site for regenerative purpose. They are responsible for both closing up the open laceration and repair tissue injury to the very last stage. Their number increases until they predominate the area. At the wound edge fibroblasts gather and differentiate into myofibroblasts stimulating contraction and wound closure [100]. To restore structure and function to the damaged tissue, fibroblasts produce new matrix such as collagen, elastin and proteoglycan along with degrading provisional one. Fibroblasts are the major source of MMPs that degrades extracellular matrix [101]. These MMPs are capable of digesting entire extracellular matrix components [102, 103].

Accordingly, all constituents of exogenous implant that are substrate specific to the secreted MMPs will be degraded along with ECM as a part of the regeneration process. If implants does not cause prolonged detrimental inflammation, the principle cell type that interacts with it is most probably the fibroblasts.

In order to develop a prototype that resembles the physiological condition and keep the assay practical, fibroblast is the only one cell type used. They perform important function in wound healing, are widely utilized in research, are commercially available, and are relatively easy to purchase and maintain. The cell line utilized in this research is the standard fibroblast cell line, NIH-3T3, a cell line established since 1962 from Swiss albino mouse embryo tissue [104]. It is very robust, stable and it is relatively easy to culture in vitro. From our consideration, it is the suitable cell line to be incorporated into our research in order to assemble a practical assay for proteinase inhibitor screening.

5.4. Cell Adhesion Support Scaffold

In this experiment, we focus on the fluorescence intensity resulting from cleavage of DQ-gelatin by viable cell secreted MMPs. Under normal physiological conditions, the level of MMP expression is very low, both in vivo and in cell culture [105]. Therefore, high concentration of cells is required to generate adequate amount of secreted MMP in order to achieve acceptable fluorescence signal emission. Fibroblasts, NIH-3T3, are anchorage dependent cells that grow in monolayer in culture. They require appropriate substrate for cell adhesion to survive [106]. By introducing porous cell anchorage substrate, we may provide more surfaces for NIH-3T3 and increase the viable cell number measured at the end of experiment.

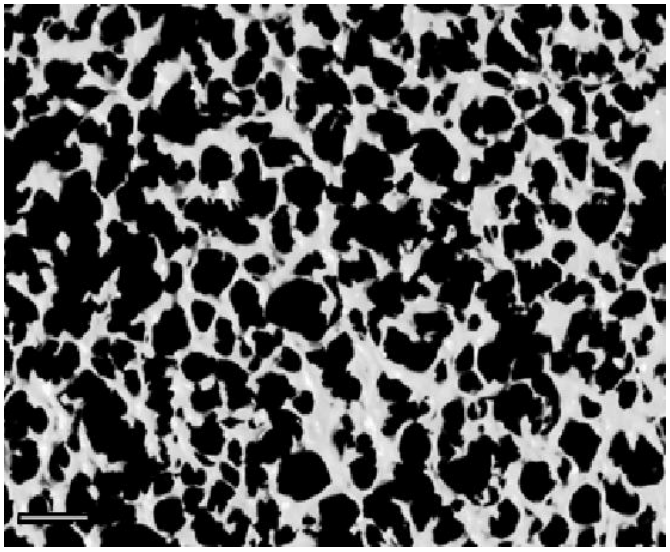

Figure 2 Cryosliced fabricated polymer scaffold, scale bar = 100 µm.

Our research group utilizes porous polymer scaffold as cell adhesion substrate in many projects [107]. The low cost and simple to fabrication scaffold is prepared by pouring aqueous free polyether-based thermoplastic polyurethanes (TPUs) solution into soft rubber mold filled with sugar. The solution seeps through space between sugar grain and fills the mold, creating porous structure once the sugar is dissolved out by water rinses. Data generated from analysis of the fabricated cryosectioned scaffold shows 67.31±8.84% pore area with very uniform density 59.08± 4.84 µg/mm3, indicating very uniform results when compared between each scaffolds.

From Figure2 high surface area could be observed, by comparing the dimension of pore size on the scaffold and NIH-3T3 cell, approximately 50 – 80 µm, pore size is wide enough for 3T3 to grow between the connected empty spaces. Therefore, the developed porous structure within the scaffold creates larger surface within the same experimental volume providing more area for fibroblast to adhere, thus are able to increase the number of viable cells remaining after

experiment. Despite the attractive potential, addition of scaffold into our assay makes the assay preparation process more complicated. During assay development, we have also conducted experiments to observe whether NIH-3T3 could be maintained without scaffold. The experiments were prepared to have one set containing scaffold and the other not containing scaffold to see the comparison. MTT assay was performed to confirm cell viability after these experiments.

5.5. MMP Inhibitor TIMP-1 and BB-94

Degradation of protein-based implant is modulated by the same process of (granulation tissue) ECM remodeling, MMPs-catalyzed hydrolysis. Matrix metalloproteinases or MMPs are a family of structurally related zinc-dependent enzyme, collectively capable of digesting all components of ECM [14, 15]. The natural inhibitor of MMPs includes the tissue inhibitors of metalloproteinases (TIMPs), α1-proteinase inhibitor and α2-macroglobulin. TIMPs are the major endogenous MMP inhibitor in tissue. They maintain the balance between ECM deposition and degradation in physiological and biological process [16]. TIMP bind to highly conserved active zinc-binding sit of MMPs at molar equivalence and suppress proteolytic activity. So far, 4 members of the TIMP family has been characterized; TIMP-1, TIMP-2, TIMP-3 and TIMP-4. Although different TIMPs bind to different MMPs with different affinity, both TIMP-1 and TIMP-2 are capable of inhibiting all known MMPs [16]. While in general TIMP plays inhibitory role, at low concentration, TIMP-2 enhances the activation of MMP-2, there by raises proteolytic activity.

In a healthy tissue, TIMP concentration normally far exceeds MMP concentration, limiting proteolytic activity to only focal pericellular sites. Although the situation of TIMP and MMP expression in injured tissue is complicated and not fully understood [68], the activity of MMP is critical in wound healing. MMP is required for debridement, cut through fibrin clot and remodeling (granulation tissue) ECM once those migrated cells populates the wounded area. As an example, collagenase activity has been shown to quickly be induced and up-regulated at the wound edge [108], during cellular infiltration of fibrin clot [72], persist during wound healing and cease after the end of re-epithelialization [109]. Different MMPs is expressed and regulated differently during these events [102].

As MMP expressions are elevated in most human tumors [110], MMP has been held as promising target for cancer therapy for over 30 years [111]. So far, large number of drugs targeting MMP has been developed to impede metastasis and angiogenesis during tumor invasion [112]. Many drugs have shown compelling results in animal studies [111]; unfortunately, most fail later during human clinical trials [110,113,114]. One of the major postulated reason issues is that the synthesized MMP inhibitors are broad-spectrum chelator, incapable of discriminating between different zinc-dependent proteases. Because our aim is not to identify the best MMP inhibitor but to assemble an assay capable of discerning MMPi potency, therefore, the only requirement for selecting our test inhibitors would be that they do not cause cells apoptosis. BB-94 is one of those synthesized MMP inhibitors that has many successful cases in animal studies [115-118] and is the first MMPi tested in Phase I studies [119]. The clinical trial has continued to Phase II in Europe [120] but Phase III has been discontinued because of slow patient accrual [121]. Because of its many successful cases in vivo,

it is chosen as our test MMP inhibitor along with TIMP-1 that has the inhibition spectrum over all known MMPs. And by introducing MMP inhibitors, we hypothesize that the extent of proteolysis of DQ-gelatin in our assay will be reduced.

The selected range to test out MMP inhibitors for our experiment is based on the estimate value of the MMP expression level in tissue, and the IC_{50} value which indicates drug's effectiveness. In normal wound, the approximate collagenase expression is 0.1-1.3 µg/mL of wound fluid with the average of 87 µg/mL. Because TIMP-1 binds to MMP at molar equivalence and that TIMP-1 is a costly reagent, our test range is 0.1-2 µg/mL. BB-94, or batimastat, is a potent broad spectrum MMP inhibitor which under physiological condition inhibits MMP with IC_{50} value in nM range; MMP-1(3 nM), MMP-2 (4 nM), MMP-3 (20 nM), MMP-8 (10 nM) [119, 123] and MMP-9 (10 NM) [123]. According to FDA, IC_{50} is the drug concentration require for 50% inhibition of specific biological process in vitro. Therefore, our test range for BB-94 is 20-1000 nM.

5.6. Cell Viability Testing

To imitate implant degradation in vivo, the signal that we are interested in is the signal produced by viable cells. Therefore, it is imperative to verify the estimates of how many cells remain viable throughout the assay. The determination of viable cell number is use in many types of research such as drug testing, cytotoxicity test and biologically active compound screening. One of the most versatile assays commonly used these days is the MTT assay [124]. It involves the conversion of the main assay component (3-[4,5-dimethylthiazol-2-yl]-2,5-diphenyl tetrazolium bromide) or MTT by mitochondrial dehydrogenases of viable cells [125-127]. The enzyme

cleaves the tetrazolium ring, transforming yellow soluble MTT into purple insoluble formazan crystals which dissolves in acidified isopropanol and the purple solution may then be measured spectrophotometrically using plate reader set to read absorbance at wavelength 570 nm. The higher the optical density, the higher the viable cell number counts. By preparing standards with known number of viable cells the information from absorption data can be interpreted.

As this simple, yet accurate method is performed as the last step our MMP inhibitor screening assay to ensure the estimate number of viable cells are at acceptable level. Our assay is set to optimize MTT test measurements and avoid components that interfere with the process. MTT assay yields highly sensitive result at cell concentration up to 10^6 cells/100 µL media. The sensitivity may lower with the increment of cell number, high protein concentration, presence of phenol red and extended incubation time of MTT with viable cells [128]. Therefore, the growth media in our assay uses phenol red free DMEM/F-12 media instead of regular formulation, exclude addition of FBS and the cell viability testing is conducted outside this process is conduct outside the original 96-well experimental vessel with the incubation time of 4 hours.

6. Experiment Setting

Our assay takes place in 96-well plate setting. The total reaction volume of 200 µL in our experiment may consist of DQ-gelatin solution dissolved in buffered fibroblast growth media, fibroblast and MMP inhibitor of choice. Signal optimization process is performed to achieve the highest signal-to-noise ratio while retaining high NIH-3T3 viability (detail discussion is reported in Chapter 3). We assume that, under optimized condition, the effect of inhibitor will be most pronounced. From previous experiments (data not shown) evaporation tremendously affected fluorescence measurement. Therefore, the outer most rows are not used as experimental vessels but are filled with sterile filtered DI water to reduce the evaporation of other inner wells of the 96-well plate. Fluorescence emission increases as DQ-gelatin is broken down and is used as indicator of gelatin degradation. The more potent the inhibitor, the less fluorescence is generated.

In general, a reliable assay generates a strong signal as a result of the target reaction occurrence. Thus, Signal optimization process is performed to achieve most distinctive fluorescence signal possible compared to emitted background while retaining high NIH-3T3 viability. The concentration of DQ-gelatin and fibroblast were varied to see the best concentration that produce highest signal-to-noise ratio. The experiments were conducted in 2 different settings; one having the cell adhesion support scaffold while the others don't, in order to examine whether the scaffold is a required component in the assay.

After the optimal condition to generate considerable fluorescence emission while retain high NIH-3T3 viability is obtained, It is used to assemble our cell based assay and test out MMP inhibitor efficacy. MMP inhibitor is only used after the assay has fully been developed.

7. Conclusion

Now a day, a large variety of protein-based biomimetic material has been used in a wide range of applications [129]. Despite their great potential, after implant majority of those materials degrades at a faster rate than the body could regeneration. Thus, lifetime prolongation of protein based materials may be a practical way to improve the implants therapeutic efficacy. In general, degradation of protein based implants take place in a similar manner as ECM remodeling, which is by MMP catalyzed hydrolysis. By inhibiting proteolysis activity of these MMPs, the implant retention time under physiological condition may be extended.

The purpose of this research is to assemble a cell-based MMP inhibitor screening assay prototype that resembles protein-based implant breakdown in vivo. As the dominant cell type at implant site, fibroblast is selected to be used as MMP source. It is cultured in presence of DQ-gelatin, a heavily fluorescence labelled gelatin that gives off fluorescence emission proportional to the extent of its degradation. To investigate the effect of MMP inhibitor, the substance is introduced into the culture containing fibroblast and DQ-gelatin. After specific period, the emitted fluorescence signal is measured. The efficacy of the MMP inhibitor is obtained by comparing how much signal is reduced as the result of MMPi addition.

Living tissue compose of viable cells, therefore in our assay, high cell viability must be maintained throughout the testing period. Because fibroblasts require substrates to survive and normally grow in monolayer in vitro, cell adhesion support scaffold is included into our assay. Cell viability test is conduct after every fluorescence-signal measurement to ensure fibroblasts are still viable after specified period.

Hypothesis: We believe that our assay could detect the inhibitory effect of MMPi on viable cell modulated protein degradation.

Approach: Fibroblast, NIH-3T3, is cultured in presence of DQ-gelatin which emits fluorescence corresponding to how much it has been broken down. The efficacy of MMP inhibitor is determined from how much fluorescence signal reduction take place as a result of that inhibitor.

CHAPTER 3: NOVEL ASSAY DEVELOPMENT

1. Rationale

Our aim is to assemble a cell-based assay capable of evaluating MMPi efficacy on delaying rate of proteolysis. As our assay is designed to mimic the degradation of protein-based materials after implant, the signal of our interest is the fluorescence signal generated from breakdown of DQ-gelatin by living cells thus; NIH-3T3 must remain viable after signal measurement. In this stage of novel assay, there are 3 main aspects of concern (1) the difference in level of generated signal from background fluorescence (2) cell viability and (3) practicality of the assay. An assay and produce high signal-to-noise ratio generated from cellular activity of viable cells that is easy to assemble is most desired.

It has been reported that cells in unstimulated culture express low level of MMP [105], therefore, high number of cells may be required to generate significantly distinct signal from the background. But as more cells are inserted into experimental vessel, less area is available for cells to adhere and nutrients are consumed within shorter period, assay optimization process is necessary to identify highest seeded cell number that could be seeded and maintained until the assay is complete. DQ-gelatin concentration and experiment time is also varied to find the best condition that gives the most recognizable signal against background fluorescence.

We have considered looking into stimulating MMP production of fibroblast in culture. Although MMP expressions can be induced by various exogenous signal such as cytokines and growth factors [105, 130], specific substance up-regulate specific MMPs, e.g. IL-1, EGF, and bFGF stimulates the production of MMP-1 and MMP-3 [130, 131] and each MMP has different

activity towards different substrate and may induce other cellular responses that are not associate with proteolysis. We have not found a substance to stimulate MMP production without changing cellular response in other aspects. Thus the act of MMP production induction itself creates the artifact. Therefore, our best option remains only to vary those conditions mentioned above, namely; the seeded cell number, fluorescence-substrate concentration and incubation time.

Fibroblasts are anchorage dependent cells; by providing less than adequate surface area for cell adhesion, those fibroblasts may undergo apoptosis before the end of experimental process. For this reason, scaffold for cell anchorage is introduced into our prototype. We are aware that by having scaffold as a component we reduce the practicality of our assay preparation, despite the ease of fabrication and economical production cost. To prove the scaffold necessity, experiments for signal optimization were conducted in 2 settings; a) without scaffold and b) with scaffold. After each fluorescence measurement, MTT cell viability assay was conducted to determine the number of viable cells.

The optimal condition we aim to identify is the condition most convenient to prepare, generate most dissernable signal while retaining the majority of NIH-3T3 population. Because optimization of one desired aspect may post negative effect on others, each factor effecting signal-to-noise ratio, cell viability and the practicality of the assay as important correlating factors that cannot be considered separately. Assay optimization process must be done to investigate the signal trend caused by different factors and the most appropriate condition to use in order to assemble or cell-based MMP inhibitor screening assay.

2. Methodology

2.1. Cell Adhesion Support Scaffold

The porous scaffold for cell adhesion support was fabricated by pouring polyurethane solution into sugar filled soft silicon rubber mold. The size of each scaffold was based on the dimension of each well in 96-well plate. To prepare the rubber mold, 3/16" hole was punched into 1/8" thick soft silicone rubber sheet (McMaster-Carr) using hole-puncher. Moist sugar was prepared by mixing 10g of sugar with 200 µL of deionized water. The sugar was pressed into the rubber mold and placed in 75°C oven to dry. Polyurethane solution was prepared by mixing 1 gram of Tecoflex SG80-A (Thermedics) per 10 mL of dimethylacetamide, DMAc (Alfa Aesar), in round bottom flask. The mixture was placed on hot plate to dissolve; the temperature was set to approximately 60 °C with 400 rpm stirring. Once the polyurethane was dissolved, it was poured drop-wise onto the sugar filled rubber mold. Dry sugar was sprinkled over the mold to remove excess polyurethane solution then the sugar was leveled at the brim of the mold by shaving off sugar outside the 3/16" cavity. The mold was carefully placed into container filled with deionized water and was left overnight to dissolve out sugar forming porous polyurethane scaffold. The scaffolds were thoroughly rinsed by constantly stirring scaffold in deionized water for 12 hours. Rinsing was repeated 3 times to ensure removal of cytotoxic DMAc. The scaffold was placed in 75% ethanol for sterilization and was washed in DPBS (Gibco) 3 times before coating with 20 µg fibronectin (Gibco) per 1 mL sterile filtered deionized water overnight to facilitate cell adhesion.

2.2. Cell Culture and Propagation of NIH-3T3

Cryopreserved NIH-3T3 (ATCC) were thawed, transferred to 15 mL centrifuge tube (VWR), added with 10 mL of DMEM/F12 media (Gibco) and centrifuged at 300 rpm for 5 minutes. The supernatant was aspirate to remove DMSO from the cryopreservation media. Cell pellets were suspended in fibroblast growth media (DMEM/F12 media (Gibco) supplemented with 10% fetal bovine serum (Gibco), 1% glutaMAX (Gibco) and 25 µg/mL gentamicin (Gibco)) and transferred to T-75 tissue culture flask (VWR). NIH-3T3s were maintained under standard condition (5% CO_2, 95% humidity at 37°C). When reach confluence, NIH-3T3s were treated with 0.25% trypsin-EDTA (Gibco). Trypsinization was stopped by addition of growth media, centrifuged and resuspended. Cells were expanded using 3-6 split ratio for each passage until the desired number of cells was obtained. All procedure were carried out under strict aseptic conditions.

2.3. Signal Optimization

Signal optimization experiments took place in tissue culture treated black 96-well plate (VWR). The total reaction volume of 200 µL in the experiment may consist of DQ-gelatin solution dissolved in buffered fibroblast growth media, fibroblast and MMP inhibitor of choice. 10X reaction buffer was prepared using sterile filtered 0.5 M Tris-HCl, 1.5 M NaCl and 50 mM $CaCl_2$. 1X reaction buffer is prepared by combining growth media, which compose of phenol red free DMEM/F12 (Gibco) supplemented with 1% glutaMAX (Gibco) and 25 µg/mL gentamicin (Gibco), with 10X reaction buffer in 9:1 ratio and was used for diluting DQ-gelatin and cell suspension. NIH-3T3 were treated with 0.25% trypsin-EDTA (Gibco) for cell detachment then stopped with growth medium. Cell suspension was centrifuged at 300g for 5 minutes. The

supernatant were aspirate out and the cell pellets were re-suspended in reaction buffer into high concentration cell suspension ready for seeding. In this signal optimization process, 2 sets of similar experiments are conduct; setting a) using scaffold and setting b) not using scaffold.

2.3.1. Setting a)

In setting a) Cells were seeded into 96-well plates at 0.002, 0.0042, 0.014, 0.035, 0.1, 0.4, 0.8 and 1.2 million cells per well. All wells were used except the outer most rows. DQ-gelatin was dissolved in reaction buffer and transfer to 96-well plate to have final concentration of 5, 10, 25 and 50 µg/mL. The total reaction volume in each well is 200 µL. Each condition was prepared in triplicated. This preparation is repeated in four 96-well plates for four time-points measurement. After the four plates were prepared and the outer most rows is filled with sterile filtered deionized water, they were wrapped in tin foil to prevent light exposure. The plates were transferred into incubator and kept under standard tissue culture conditions for 3, 7, 10 and 15 hours. At the designate time, the emitted signal is read using plate reader set to read florescence with absorption maxima approximately at 495 nm and emission maxima approximately at 515 nm.

2.3.2. Setting b)

In setting b) the experiment were conducted in similar manner with setting a) with a few exceptions that cells adhesion support scaffold were used. The 2 fibronectin coated scaffolds were placed in each well of 96-well plate and aspirate dried. NIH-3T3 were seeded at 0.1, 0.2, 0.4 and 0.8 million cells per well and the preparation is repeated in three plates for three time-points measurement after 1, 3 and 5 days.

2.4. NIH-3T3 Viability Testing

After every fluorescence measurement, the percent viability of NIH-3T3 for each condition was quantified by MTT (3-(4,5-Dimethylthiazol-2-yl)-2,5-Diphenyltetrazolium Bromide) assay utilizing the conversion of yellow MTT to purple formazan by active mitochondrial dehydrogenase in viable cells according to the manufacturer protocol (Sigma) with minor modifications. Briefly, standard with known cell number was prepared and transferred separately to 24-well plate along with all content from each well in 96-well plate. 100 µL of 12 mM MTT solution, prepared by dissolving MTT in sterile DPBS (invitrogen), was inserted to each well follow by 700 µL of DMEM/F12 without phenol red. The plate was incubated at 37°C for 4 hours, then 1 mL of formazan dissolving solution, 0.1 N HCI dissolved with 10% Triton-100 in anhydrous isopropanol, was added to each well and mix thoroughly to solubilize formazan. The absorbance of the purple formazan solution was measure by plate reader at wavelength 570 nm. Viable cell number was estimated using prepared standard curve.

2.5. Mathematical Model Construction and Statistical Analysis

Numerical data for fluorescence signal and MTT viability assay were assessed by JMP Pro11/ statistical analysis package. Data were compiled to visualize how DQ-gelatin concentration, seeded cell number and reaction run-time effect the signal-to-noise ratio and cell viability. Mathematical model were constructed based on those data to find the optimal condition to achieve distinct signal while fibroblasts still remain viable.

As for statistical analysis, ANOVA was performed to determine statistical significance between groups, i.e. inhibitor or concentration, followed by Tukey test once significant difference was detected. Statistical significance was considered at p values of less than 0.05.

3. Result and Discussion

To find the specific condition that would produce highest signal-to-noise ratio while maintaining high cell viability, assay optimization process was conducted. The experiments were prepared in two settings; setting a) without scaffold and setting b) with scaffold. Seeded cell number, DQ-gelatin concentration and incubation time were varied. At designate time, florescence was measured and MTT assay was performed to estimate cell viability. The emitted fluorescence is converted into signal-to-noise ratio to signify how different the cell-related emitted signals are from the background fluorescence. Absorbance from MTT assay was converted to cell number estimates based on the known prepared standards. The signal-to-noise ratio and NIH-3T3 viability were combined and assessed using JMP pro11 formed into mathematical model to obtain optimal condition that generate high signal-to-noise ratio while keeping the cells alive. From the generated model and statistical analysis, the factors and their significance on signal-to-noise ratio and cell viability could be illustrated.

3.1. Setting a)

Analysis of Variance

Source	DF	Sum of Squares	Mean Square	F Ratio
Model	9	56.847144	6.31635	484.8054
Error	374	4.872707	0.01303	**Prob > F**
C. Total	383	61.719850		<.0001*

Figure 3 Analysis of variance. ANOVA of setting a) signal-to-noise ratio in signal optimization process; treating each specific condition; concentration and cell seeding number as one treatment (n=3, $p<0.05$)

Analysis of variance suggests that there are significant differences resulting from varying experiment preparation conditions; seeded cell number, DQ-gelatin concentration and incubation time. From the complied signal-to-noise ratio, mathematical model or prediction plot with R^2 value of 0.92 were constructed. In statistical analysis, R^2 provides measure of how well the model represents the data in terms of proportion of total variation of outcomes explained by the model, ranging from 0-1 [133]. With R^2 of regression plot equivalent to 0.92, the ability of the constructed model to predict real value is relatively very accurate.

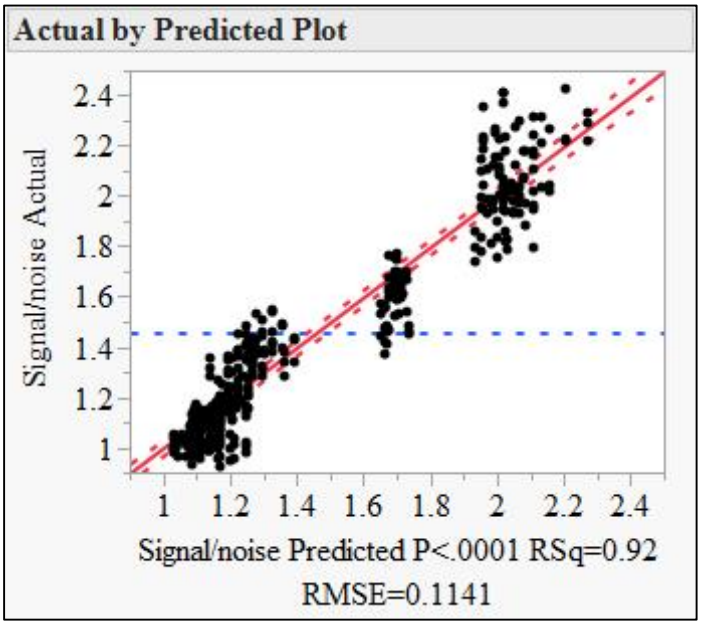

Figure 4a Actual by predicted plot. All actual collected signal/noise data are displayed as black dots against red predicted plot.

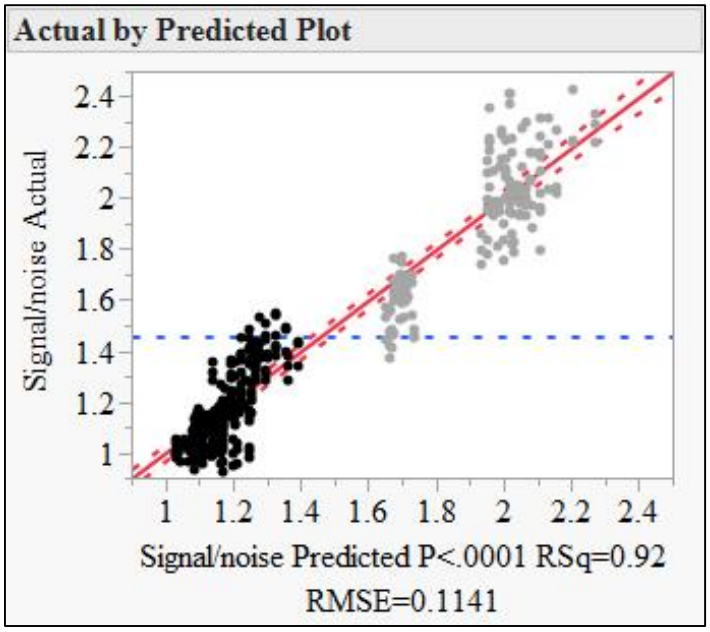

Figure 4b Actual by predicted plot. Signal-to-noise ratio from experiments with seed cell number between 0.002-0.1 million cells.

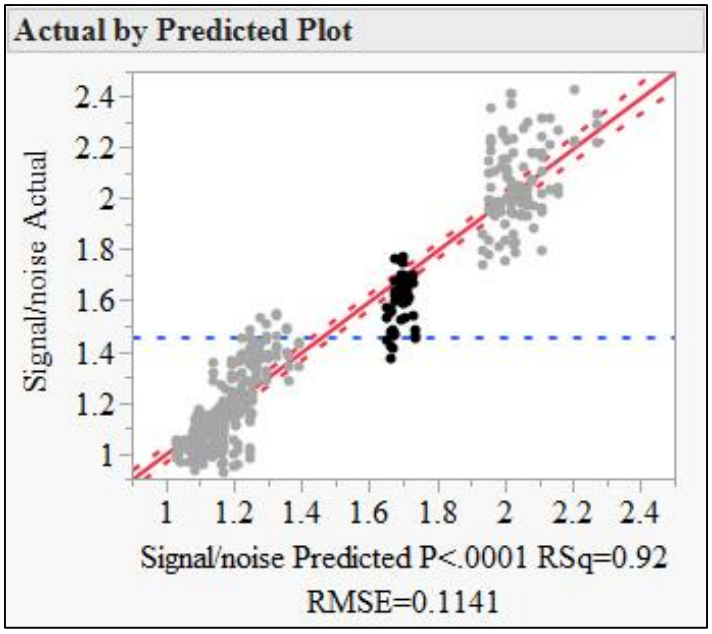

Figure 4c Actual by predicted plot. Signal-to-noise ratio from experiments with seed cell of 0.4 million cells.

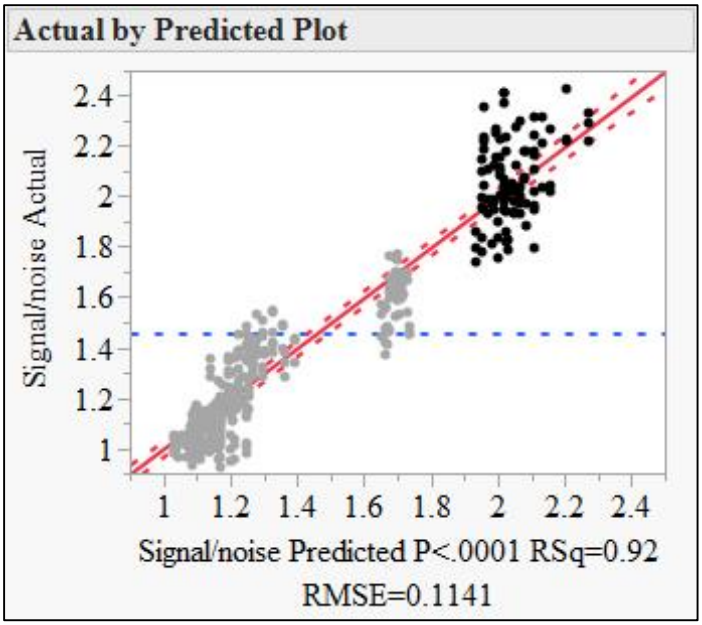

Figure 4d Actual by predicted plot. Signal-to-noise ratio from experiments with seed cell number between 0.8-1.2 million cells.

Figure 4 shows actual signal-to-noise ratio from collected data as round dots plotted against the established mathematical model displayed in red line. The signal-to-noise ratio of experiments with seeded cell number equals to 0.002-0.1 million cells, 0.4 million cells and 0.8-1.2 million cells are presented as black dot on figure 4b), 4c) and 4d) respectively. From the figure, it could be concluded that as the number of seeded cell increases, the higher signal-to-noise ratio produced.

The predicted plot or the mathematical model generated from collected signal-to-noise ratio via JMP consist of 3 experimental variables; seeded cell number, experiment time and DQ-gelatin concentration. Statistical analysis of the mathematical model (Figure 5) shows the extent of significance post by each variable term on signal-to-noise ratio generation. Probability values

shown in orange are highly significant while the values shown in red are significant at 0.05 level. By far, the number of seeded cell place highest impact on signal-to-noise ratio production. The terms shown below are used to construct our mathematical model displayed on figure 5. Once included in the model, terms with higher significance will cause predicted value to be closer to the collected data, resulting in constructed model with higher R-square value.

To investigate how each experimental variable; seeded cell number, DQ-gelatin concentration and incubation time, affects the trend of signal-to-noise ratio, the generated data were plotted against varying value of 2 selected factors in 3 dimensions. In Figure 6a) on horizontal axis are the seeded cell number and the DQ-gelatin concentration. The signal-to-noise ratio data are shown as black dots against the green sheet model. The vertical lines of dots are data generated at the same seeded cell number and DQ-concentration with different incubation time. The higher signal-to-noise ratio is the shorter the incubation time (data not shown). Similarly, in Figure 6b) the seeded cell number and incubation time are displayed on horizontal axis. The vertical lines of dots are signal-to-noise ratio produced by experiments with same seeded cell number and incubation time but at different DQ-concentration.

The prediction profiler enables a clear visualization of how each experimental variable affects the trend of signal-to-noise ratio at specific condition. On Figure 6 c), the trend at conditions that produce the highest signal-to-noise ratio is shown. The shortest incubation time, highest DQ-gelatin concentration and largest number of seeded cell provides the best/most preferable condition of signal optimization. The steepness of the trend shows how much change in that

variable affects the signal-to-noise ratio. The effect of variation in seeded cell number on signal-to-noise ratio is by far greater than that of concentration and incubation time.

Parameter Estimates

Term	Estimate	Std Error	t Ratio	Prob>|t|
Intercept	1.1945018	0.016469	72.53	<.0001*
Hours	0.0032855	0.001349	2.43	0.0154*
Conc	-0.001854	0.000458	-4.05	<.0001*
Seeded Cell #	1.2339344	0.025864	47.71	<.0001*
(Hours)*(Hours)	-0.000304	0.000347	-0.88	0.3821
(Hours)*(Conc)	-0.000119	0.000076	-1.56	0.1196
(Conc)*(Conc)	9.2784e-5	2.857e-5	3.25	0.0013*
(Hours)*(Seeded Cell #)	-0.020221	0.003139	-6.44	<.0001*
(Conc)*(Seeded Cell #)	0.0043062	0.000786	5.48	<.0001*
(Seeded Cell #)*(Seeded Cell #)	-0.78413	0.046993	-16.69	<.0001*

Figure 5a Sorted parameter estimates and mathematical equation of constructed model. 9 terms of parameter estimates that are used to generate signal/noise ratio model

Sorted Parameter Estimates

	Term	Estimate	t Ratio	Prob>|t|
1	Seeded Cell #	1.2339344	47.71	<.0001*
2	(Seeded Cell #)*(Seeded Cell #)	-0.78413	-16.69	<.0001*
3	(Hours)*(Seeded Cell #)	-0.020221	-6.44	<.0001*
4	(Conc)*(Seeded Cell #)	0.0043062	5.48	<.0001*
5	Conc	-0.001854	-4.05	<.0001*
6	(Conc)*(Conc)	9.2784e-5	3.25	0.0013*
7	Hours	0.0032855	2.43	0.0154*
8	(Hours)*(Conc)	-0.000119	-1.56	0.1196
9	(Hours)*(Hours)	-0.000304	-0.88	0.3821

Figure 5b Sorted parameter estimates and mathematical equation of constructed model. The terms are presented orderly with respect to their significance on model-fitting.

1.162240 + (1.347825 * Seeded Cell #) + [(-0.850079) * (Seeded Cell # - 0. 281786)^2] + [(-0.0194441) * (Hours - 8.735499) * (Seeded Cell # - 0.281786)] + [(0.003620) * (Conc - 22.436195) * (Seeded Cell # - 0. 281786)] + ((-0.001693) * Conc) + [(0.000080) * (Conc - 22. 436195)^2] + (0.002814 * hours) + [(-0.000122) * (Hours – 8.735499) * (Conc - 22.436194)] + [(-0.000302) * (Hours - 8.735499)^2]

Intercept + [(1.347825) * 1] + [(-0.850079) * 2] + [(-0.194441) * 3] + [(0.003620) * 4] + [(-0. 001693)* 5] + [(0.000080) * 6] + [(0. 002814) * 7] + [(-0.000122) * 8] + [(-0.000302) * 9]

Figure 5c Sorted parameter estimates and mathematical equation of constructed model. Mathematical model for signal-to-noise ratio prediction. Term Seeded Cell # refers to seeded cell number, Hours refer to incubation time and Conc refers to DQ-gelatin concentration

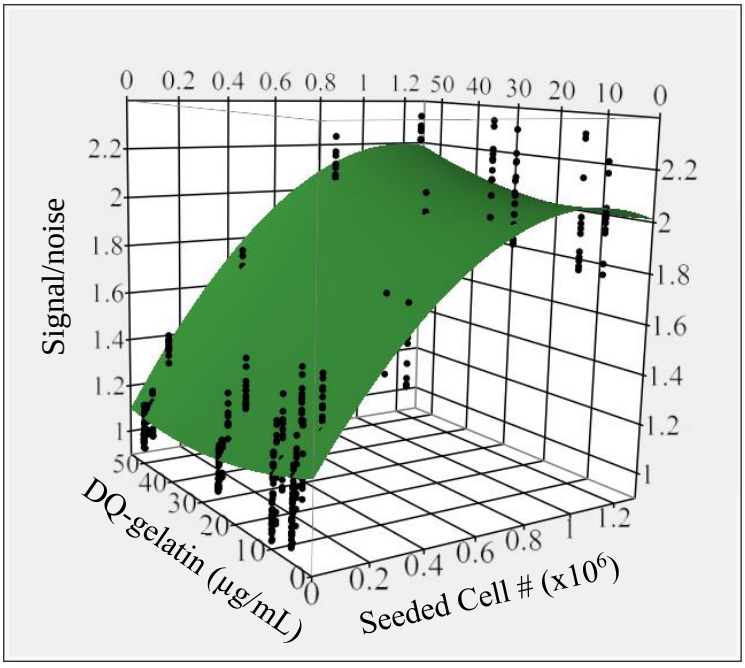

Figure 6a 3-Dimensional plot of signal-to-noise ratio. Signal-to-noise ratio data is plotted against seeded cell number and DQ-gelatin concentration

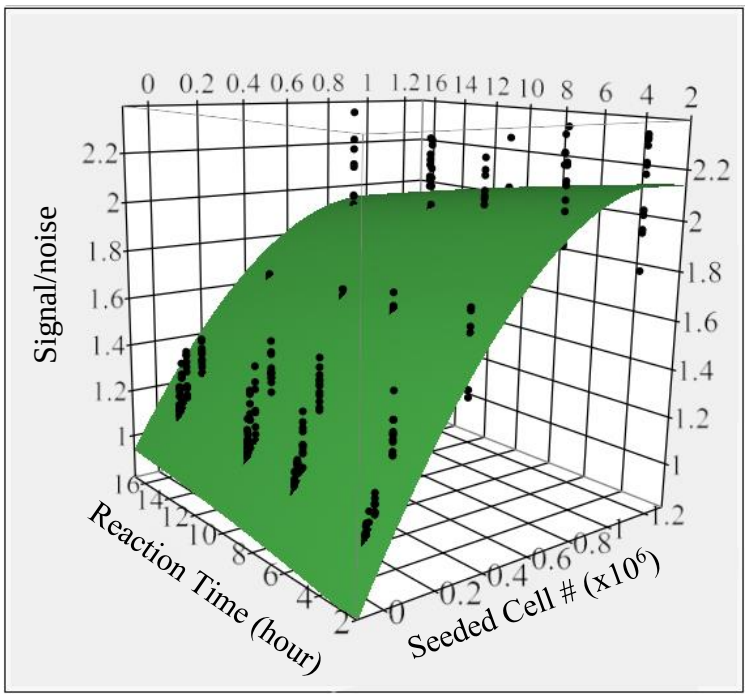

Figure 6b 3-Dimensional plot of signal-to-noise ratio. Signal-to-noise ratio data is plotted against seeded cell number and incubation time.

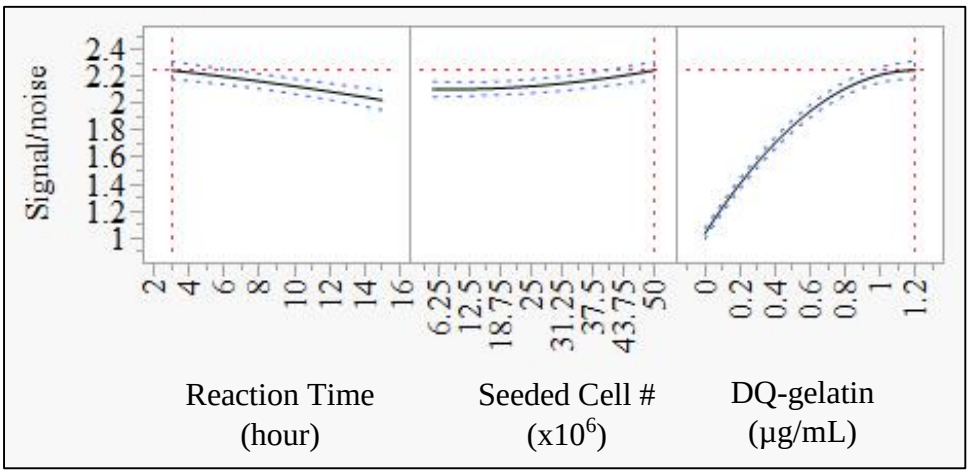

Figure 6c 3-Dimensional plot of signal-to-noise ratio. Prediction profiler set at the optimal condition for signal generation.

After the signal to noise ratio trend has been established, we identify the significant difference within each variable by performing Tukey test, shown in Figure 7 ($n=3$, $p<0.05$). Signal-to-noise ratio barely increase as incubation time is prolonged and does not linearly vary in according to DQ-gelatin concentration but significantly escalates as seeded cell number is increased. Despite the modest value of signal-to-noise ratio, all conditions of seeded cell number produce significantly distinct signal-to-noise ratio from the no cell control. This result confirms the reliability of our assay.

In conclusion, the signal-to-noise ratio generated from DQ-gelatin break down is largely governed by seeded cell number. Their significant influence is supported by the 2-dimensional plot in Figure 3, parameter estimates in Figure 4, the slope of signal-to-noise ratio trend in figure 6 and from statistical analysis. Signal-to-noise ratio is also affected by DQ-gelatin concentration and incubation time but in a lesser extent. The result from constructed model may differ a little from statistical analysis in figure 7. This is because the model shows the prediction at specific condition, ($n=3$), e.g., at certain DQ-gelatin concentration, seeded cell number and incubation time but in Tukey-test, one condition of one vaiable is fixed consequently, the information is the average of the estimate over a wide range of condtions and the signal-to-noise trend varies as the governing experimental condition changes. Therefore, if one is interested to predict signal-to-noise ratio or trend at specific condition, it would be more accurate to rely on the constructed model, figure 6, rather than the overall result separate by certain category presented by Turkey test, figure 7.

DQ-gelatin (µg/mL)

Level		Least Sq Mean
10	A	1.4363966
5	A B	1.4212470
50	B	1.3980940
25	C	1.3692600

Seeded Cell # (x10^6)

Level		Least Sq Mean
0.8	A	2.0654992
1.2	A	2.0578424
0.4	B	1.5974884
0.1	C	1.3998367
0.035	D	1.2053771
0.014	E	1.1471708
0.0042	E F	1.1056612
0.002	F	1.0773689
0	G	1.0000000

Reaction Time (hour)

Level		Least Sq Mean
15	A	1.4186605
10	A	1.4110110
7	A	1.4104448
3	B	1.3848813

Figure 7 Turkey Test analysis on each experimental viariable. Tukey test on incubation time (n=108), seeded cell number and (n=54), DQ-gelatin concentration (n=108).

Cell Viability Test

After fluorescent signal measurement, MTT cell viabiliy test is performed to estimate the number of remaining viable cells. Yellow MTT solution is converted to purple formazan crystal via components of viable cells and is measured by absorption. The approximate number of viable cell can be obtained from comparing obtained result against a standard curve. The number of viable cells are translate and presented as percentage of the initial seeded number.

Our aim is to verify usable conditions that generates high signal-to-noise ratio while maintaining high viable cell percentage. It is not our focus to study how experimental variable excerts impact on cell viability and proliferation. The produced cell viability percentage used for statistical analysis and to construct a mathematical model having each experimental variable set as non-corelating factors. The analysis of varience suggest there are significance difference between cell

viability percentage resulting from different conditions (n=3, $p<0.05$). The obtained model has the R^2 value of 0.93 showing relatively high accuracy in predicting actual percent viability.

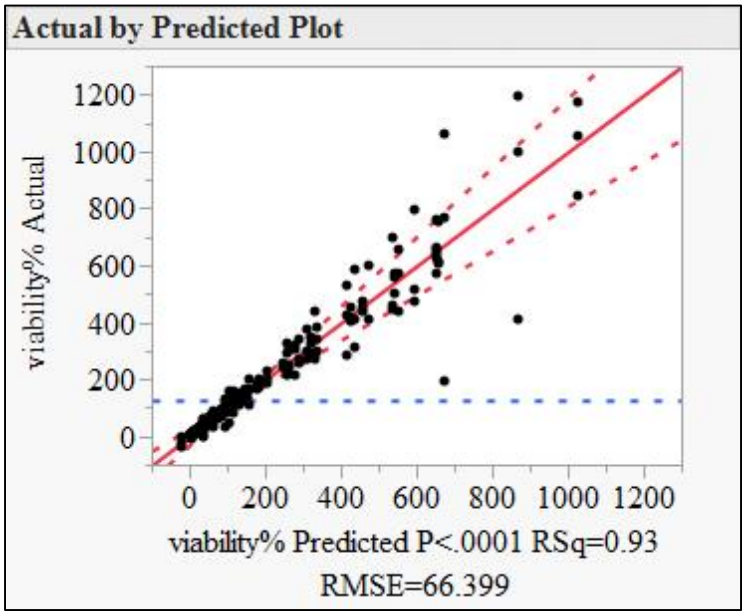

Figure 8a Statistical analysis of cell viability test setting a). Actual data plotted against predicted model as black dos against red line

Analysis of Variance

Source	DF	Sum of Squares	Mean Square	F Ratio
Model	127	15098446	118885	26.9657
Error	254	1119826	4409	Prob > F
C. Total	381	16218272		<.0001*

Figure 8b Statistical analysis of cell viability test setting a). Anova of setting a) cell viability test

Parameter Estimates				
Source	DF	Sum of Squares	F Ratio	Prob > F
Hour	3	201074.9	15.2027	<.0001*
Conc	3	753396.0	56.9620	<.0001*
Hour*Conc	9	528425.4	13.3176	<.0001*
Seeded	7	9613725.1	311.5135	<.0001*
Hour*Seeded	21	814377.4	8.7961	<.0001*
Conc*Seeded	21	1599664.4	17.2780	<.0001*
Hour*Conc*Seeded	63	1536879.7	5.5333	<.0001*

Figure 8c Statistical analysis of cell viability test setting a). Parameter estimates, displaying the significance of parameters on model fitting

Figure 9 gives a rough estimation that cell viability percentage is majorly dictated by the seeded cell number. The lower the number of cell initially seeded the higher percent viability. The over 100% value in cell viabliliy gives an indication of cell ploriferation. As the number of seeded cell is increased, the viability percentage drops. The assumtion the the cell viability percentage is largely affected by seeded cell number is also confirmed by the relatively high F-ratio in parameter estimates, Figure 8c).

To conclude signal optimization setting a), signal optimization experiment sets without scaffold, the experiment conditions that generates the our highest range of signal-to-noise ratio could not maintain a satisfactory level of cell viability while those that are capable of maintaining more than 80% viability produces less discernible signal. Therefore, although all level of seeded cell number produce statistically significant distict signal from the background, the conditions that supports cell viability produce low signal-to-noise ratio and thus we suggest finding another

alternative that could produce acceptable signal strength while keeping more cells alive throughout the course of experimental procedures.

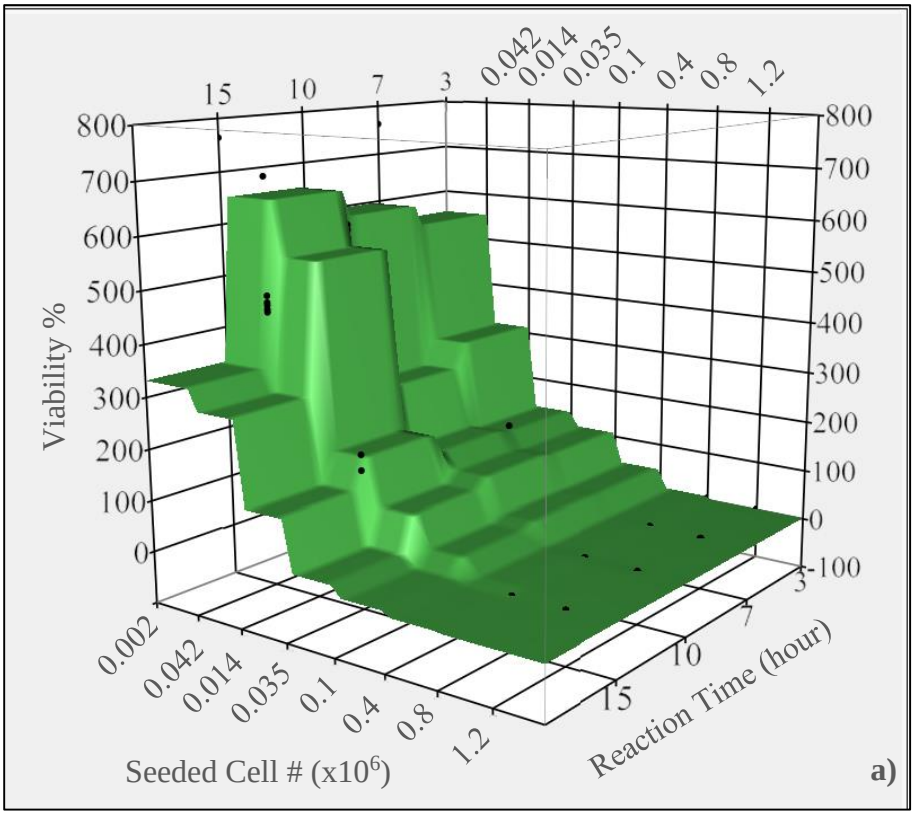

Figure 9a NIH-3T3 Cell viability percentage. Cell viability is reported in percent of the original seeded number. Viability percentage is plotted against seeded cell number and incubation time.

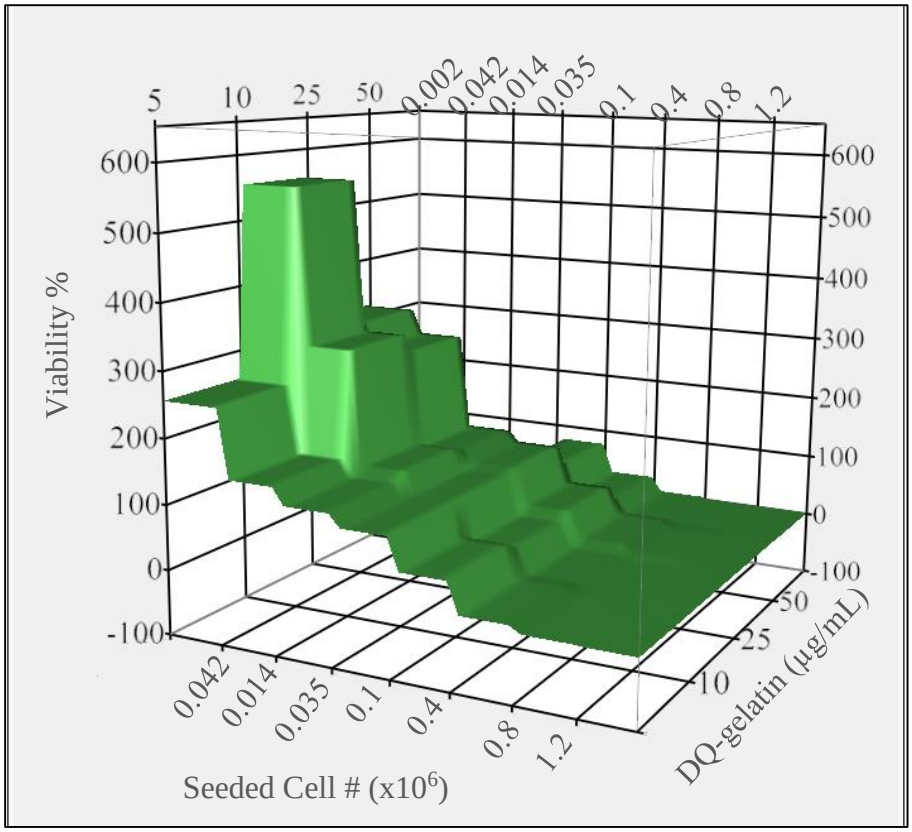

Figure 9b NIH-3T3 Cell viability percentage. Cell viability is reported in percent of the original seeded number Viability percentage is plotted against seeded cell number and DQ-gelatin concentration

Level					Least Sq Mean
0.002	A				467.54949
0.0042		B			296.09474
0.014			C		125.69955
0.035				D	80.77020
0.1				E	31.76223
0.4				E	7.25179
0.8				E	2.55261
1.2				E	1.98238

Figure 10 Turkey Test analysis on percent cell viability of different seeded cell number. Least square mean value represents cell viability percentage at the seeded cell number in milion cell. Levels not connected by the same letters are statistically different.

3.2. Setting b)

Analysis of Variance				
Source	DF	Sum of Squares	Mean Square	F Ratio
Model	9	20.427565	2.26973	64.4083
Error	127	4.475445	0.03524	Prob > F
C. Total	136	24.903010		<.0001*

Figure 11 Analysis of variance. ANOVA of setting b) signal-to-noise ratio in signal optimization process; treating each specific condition; concentration and cell seeding number as one treatment (n=3, $p<0.05$)

In these set of experiments, cell adhesion support scaffold is included into the assay to verify their positive impact on cell viability and weather they cause changes in experimental results. Analysis of varience suggest statistical significance between each group of experiments prepared by varying seeded cell number, DQ-gelatin concentration and incubation time, Figure 11 (n=3, $p<0.05$). Out of 144 conditions, 6 outliers were excluded. The constructed mathematical model from compilation of signal-to-noise ratio data and statistical analysis has R^2 of 0.82, figure 12a), which is relatively high, thus it is possible for the model to closely predict the real values experimental values. The mathematical model consist of terms listed in figure 12b), having significance on the model according to the absolute value of their t Ratios.

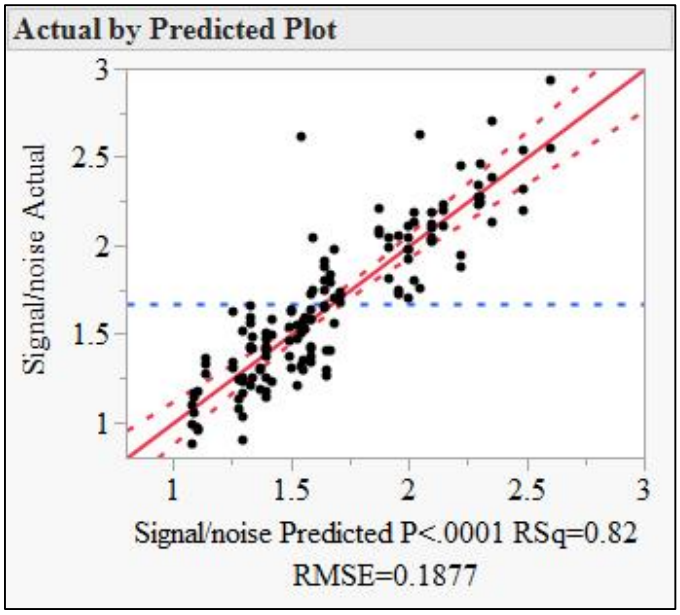

Figure 12a Mathematical model. Actual signal-to-noise data are displayed as black dots against red predicted plot.

Parameter Estimates

Term	Estimate	Std Error	t Ratio	Prob>|t|
Intercept	0.9628313	0.051919	18.54	<.0001*
days	0.1194933	0.009691	12.33	<.0001*
Seeded	1.4373933	0.083198	17.28	<.0001*
conc	0.0040321	0.001258	3.20	0.0017*
(days)*(days)	-0.038043	0.008648	-4.40	<.0001*
(days)*(Seeded)	0.2099351	0.036811	5.70	<.0001*
(Seeded)*(Seeded)	-1.945501	0.319578	-6.09	<.0001*
(days)*(conc)	0.0005425	0.000557	0.97	0.3320
(Seeded)*(conc)	0.0064007	0.00349	1.83	0.0690
(conc)*(conc)	-0.000107	7.826e-5	-1.37	0.1744

Figure 12b Mathematical model. Parameter estimates of each term that is used to generate mathematical model.

$$0.962831 + (0.119493 * \text{Days}) + (1.437393 * \text{Seeded Cell\#}) + (0.004032 * \text{conc}) + [(-0.38034) * (\text{Day-3})^2] + [(0.209935) * (\text{Day-3}) * (\text{Seeded Cell\#} - 0.370803)] + [(-1.945501) * (\text{Seeded Cell\#} - 0.370803)^2] + [(0.000543) * (\text{Day-3}) * (\text{conc} - 22.518248)] + [(0.000641) * (\text{Seeded Cell\#} - 0.370803) * (\text{conc} - 22.518248)] + [(-0.000107) * (\text{conc} - 22.518248)^2]$$

Figure 12c Mathematical model. Equation for the constructed mathematical model; Term Seeded Cell # refers to seeded cell number, Days refer to incubation time and conc refers to DQ-gelatin concentration.

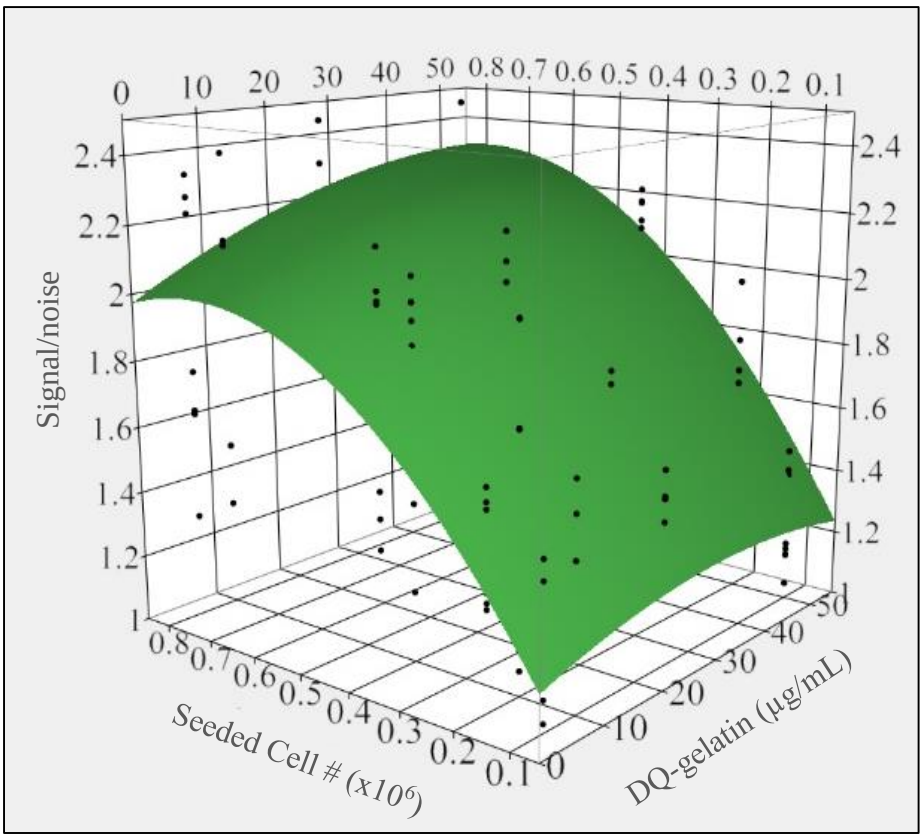

Figure 13a 3-Dimensional plot of signal-to-noise ratio. Signal-to-noise ratio data is plotted against seeded cell number and DQ-gelatin concentration

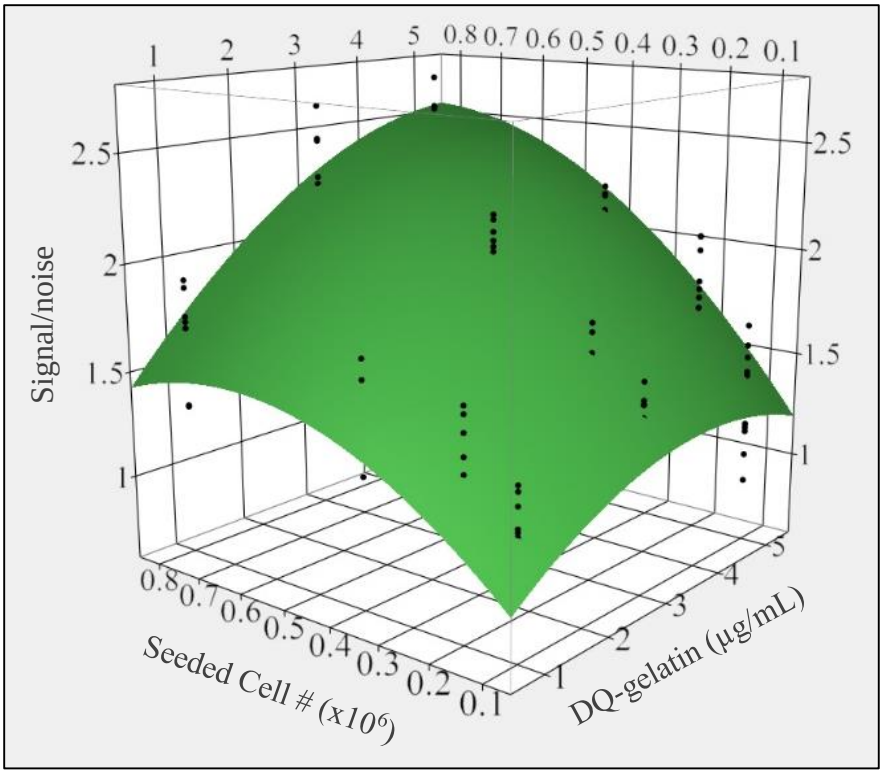

Figure 13b 3-Dimensional plot of signal-to-noise ratio. Signal-to-noise ratio data is plotted against seeded cell number and incubation time.

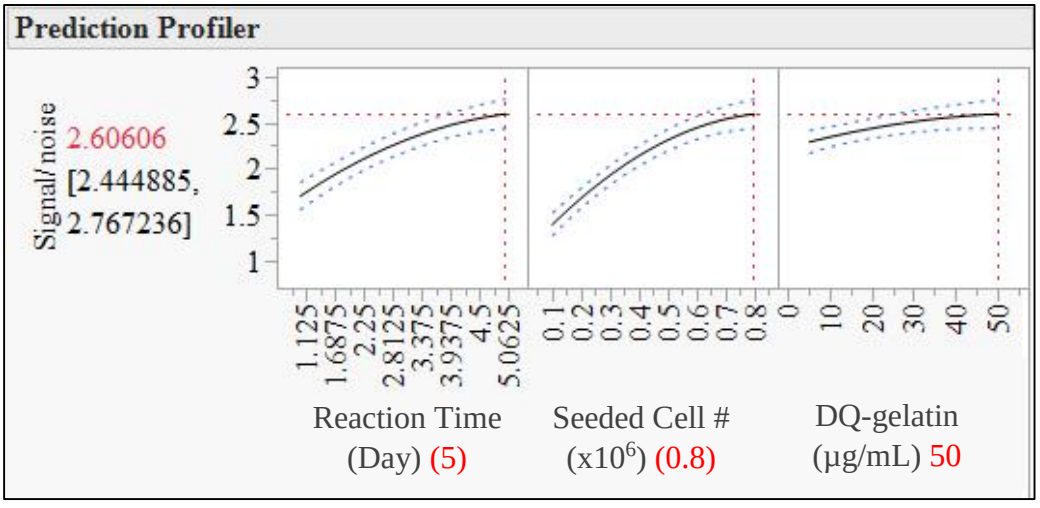

Figure 13c 3-Dimensional plot of signal-to-noise ratio. Prediction profiler set at the condition which produce highest signal-to-noise ratio. Red number indicates predicted optimal attainable value.

To study how seeded cell number, DQ-gelatin concentration and incubation time affect the signal-to-noise ratio trend, the collected data are plotted against these factors and are displayed as two 3-dimensional plots on figure 13. It is noticeable that the signal-to-noise ratio trend shifts a little as one factor is varied. For example, the effect of seeded cell number increases as the number of days and DQ-gelatin is increased. This could be visualized as the increase in steepness of the slope when comparing the trend line between day 1 and day 5, and of DQ-gelatin concentration at 5 and 50 µg/mL.

The slope increase may be caused by the more ease of access for cells when more DQ-gelatin were available, therefore, there were more opportunities for DQ-gelatin degradation to take place. Also, by prolonging the incubation period, there is longer time for cells to for cell modulated proteolysis, as a result, the effect of seeded cell number are more pronounced.

On the prediction profiler, the trend at the condition that generates the highest signal-to-noise ratio is displayed. From figure 13, the optimal condition would be the highest seeded cell, highest DQ-gelatin concentration and the longest incubation time. The statistical significance of each varied variables is verified by Tukey Test, figure 14. Changes in DQ-gelatin concentration does not cause large distinction in resulting signal-to-noise ratio while changes in all levels of seeded cell number and incubation time cause the resulting signal-to-noise ratio to be statistically different in each conditions.

Reaction Time (Day)			
Level			Least Sq Mean
5	A		1.8698359
3		B	1.7781611
1		C	1.3827147

Seeded Cell # (x10^6)			
Level			Least Sq Mean
50	A		1.7477652
25	A		1.7046598
10	A	B	1.6554068
5		B	1.5997838

DQ-gelatin (µg/mL)				
Level				Least Sq Mean
0.8	A			2.0750721
0.4		B		1.8377423
0.2			C	1.5311702
0.1			D	1.2636310

Figure 14 Turkey Test analysis result. Turkey test were performed on percent cell viability of different incubation time, seeded cell number and DQ-gelatin concentration. Least square mean value represents cell viability percentage at the condition level in million cells. Levels not connected by the same letters are statistically different.

Cell Viability Test

Following fluorescence measurement of signal optimization setting b), cell viability check was conducted. Analysis of variance shows no statistical significant difference resulting from varying seeded cell number, DQ-gelatin concentration and incubation time, (n=3, p=0.05), Figure 15. Therefore, mathematical model of viable cell percentage will not been constructed for this setting. From analysis of raw data, the viability percentage of the condition contributing to highest signal-to-noise ratio is 251.48 ± 42.44% indicating that there is more than adequate number of viable cells persisting throughout the experiment. Therefore, the concluded best condition in signal optimization experiments setting b) is the condition with seeded cell number of 0.8 million cells, 5 days incubation period and 50 µg/mL of DQ-gelatin concentration.

Analysis of Variance				
Source	DF	Sum of Squares	Mean Square	F Ratio
Model	47	1.5964e+18	3.397e+16	0.9261
Error	89	3.2642e+18	3.668e+16	Prob > F
C. Total	136	4.8606e+18		0.6074

Figure 15 Analysis of variance for cell viability of setting b) Anova on NIH-3T3 viability in signal optimization setting b); treating each specific condition; concentration and cell seeding number as one treatment (n=3, $p<0.05$). The analysis were not able to detect significant difference between each conditions

3.3. Overall Results and Discussion

From our experiments, as the incubation time is extended, the level of background fluorescence increases, therefore, our measured fluorescence data is converted to signal-to-noise ratio to maintain the consistency and to report the distinctiveness of the emitted fluorescence.

In setting a) experiment without cell adhesion support scaffold, mathematical model for signal-to-noise ratio indicates that the main contributing factor to signal-to-noise level is the seeded cell number. But because the condition that contributes to higher signal range cannot maintain satisfactory amount of cell viability, the governing mathematical model is the percent viability model, not the model for signal-to-noise ratio. From percent viability model, the predicted optimal conditions were the experiments with seeded cell number of 0.35 million cells incubated with 25 µg/mL of DQ-gelatin for 15 hours with signal-to-noise ratio of $1.23 \pm 4x10^{-2}$. This deviates a little from the actual highest signal-to-noise ratio is 1.40 ± 0.05 from experiment with seeded cell number of 0.35 million cells incubated with 10 µg/mL of DQ-gelatin for 10 hours.

The optimal condition to pick from these options is somewhat questionable. All in all, because the conditions with higher signal-to-noise ratio cannot support NIH-3T3 to remain viable, we suggest seeking other alternatives for cell-based assay assembly instead of considering for best options out of experiments from setting a).

In setting b) experiment with cell adhesion support scaffold, analysis of variance cannot detect the significance between different treatment conditions thus reliable mathematical model cannot be constructed. From rough cell viability data analysis, majority of the experiments provide considerable capacity to maintain cell viability, e.g., over 80% viability. The mathematical model for signal-to-noise ratio suggest the most suitable condition for signal optimization 0.8 million cells, 5 days incubation period and 50 µg/mL of DQ-gelatin concentration. This suggestion agrees with the actual conducted experimental condition that generates the highest signal-to-noise ratio of 2.67 ± 0.23. MTT test confirms the capacity of the cell adhesion scaffold to prevent cell apoptosis by showing viability percentage of 251.48 ± 42.44%. By comparing highest obtained signal-to-noise ratio and cell viability of setting a) and setting b), cell adhesion scaffold play role in increasing signal-to-noise ratio and maintain cell viability therefore is worth incorporating to be a part of the assay despite the reduction in practicality from assay preparation.

From all experimental condition conducted, the highest attainable signal-to-noise ratio was 2.67 ± 0.23. This small number coincides with what has been mentioned in Ravanti et al. that cells in unstimulated culture express exceedingly low level of MMPs. With minute amount of MMPs,

only small extent of florescence signal could be generated, resulting in low value of signal-to-noise ratio. Despite these concerns, the signal-to-noise ratios produced by different conditions are all statistically different from background fluorescence. These results suggest that even though those NIH-3T3S produce small amount of MMPs, it is adequate to generate statistically distinct signal and therefore, it could be concluded that cell based assay is a feasible method for semi-quantitative proteolytic degradation detection.

4. Conclusion

The objective of assay optimization process is to identify the condition that is most practical to prepare that provides the highest signal-to-noise ratio while retaining an acceptable number of viable NIH-3T3 cell. The optimization process is conduct by culturing NIH-3T3 cells in presence of DQ-gelatin which emits fluorescence signal proportional to its extent of degradation. The number of seeded cell, DQ-gelatin concentration and the incubation time is varied. The experiments in conducted in 2 sets; setting a) without cell adhesion support scaffold and b) with the scaffold. This is done to verify the necessity of the scaffold.

The highest signal-to-noise ratio of the condition in setting a) that could maintain more than 80% of originally seeded NIH-3T3 was $1.23 \pm 4x10^{-2}$ while in setting b) the highest signal-to-noise ratio is 2.67 ± 0.22. Therefore, we conclude that the cell adhesion support scaffold is a necessary component of our assay the increases the capacity to retain cell viability and enhance the signal intensity.

Because of the distinctive signal generated from cell driven DQ-gelatin breakdown and the high percentage of maintained NIH-3T3, we anticipate that a cell-based assay that resembles protein-based implant break down in vivo could be assembled. Upon introduction of MMPis the breakdown of DQ-gelatin could be and the reduction in fluorescene emission could be measured. The extent of fluorescence emission indicates the proteolytic inhibitory efficacy of the inhibitor. Based on these assumptions, MMP inhibitor screening assay could be constructed and apply to determine the suitability of the tested MMPs.

The identified condition that provides the highest signal-to-noise ratio that can maintain NIH-3T3 viability is the experiment in setting b) with seeded cell number of 0.8 million cells, 5 days incubation period and 50 µg/mL of DQ-gelatin concentration. This condition will be used in MMP inhibitor screening assay to determine the inhibitory effect that our selected MMP inhibitors possess.

CHAPTER 4: CELL-BASED MMP INHIBITOR SCREENING ASSAY

1. Rationale

After the optimal experiment condition has been determined, it is used to assemble our cell-based MMP inhibitor screening assay. NIH-3T3 is cultured on cell adhesion support scaffold at 0.8 million cells/well, in presence of 50 µg/mL DQ-gelatin with varying amount of MMP inhibitor, determined in prototype optimization. After 5 days the emitted fluorescence is measured at designate time point. This signal from culture without MMP inhibitor is used as a control to compare with emitted signal from cultures with MMP inhibitor. When the inhibitor binds to zinc binding domain of MMP, the enzyme proteolytic activity is deactivated leading to reduction in fluorescence emission because of less degradation of DQ-gelatin has taken place. From this logic, we believe the inhibitory effect of MMPi could be determined and used this quantification as means for screening potential MMPi for protein based implant lifetime prolongation.

The efficacy of the inhibitor is reported in percent reduction of fluorescence signal from culture without MMP inhibitor. The more effective the inhibitor, the lower signal is generated. Selected MMP inhibitors are added in a varied concentration to determine the optimal dosage. Cell viability assay is performed to ensure high percentage of seeded NIH-3T3 remain alive throughout the assay. Statistical analysis was performed to see the result precision, the significance between each type of inhibitor and the difference in their inhibitory effect at difference concentration.

2. Methodology

2.1. Assay Preparation

Material required, reagent preparation, fibroblast culture, scaffold fabrication, and viability assay were carried out as mentioned in the methodology section of chapter 3. MMP inhibitor screening assay experiments take place in tissue culture treated black 96-well plate (VWR). Growth media as used in signal optimization was mixed with 10X reaction buffer in 1:9 ratio to be used as reaction buffer for diluting DQ-gelatin and cell suspension. NIH-3T3 were detached, spun-down and made into high concentration cell suspension ready for seeding.

2.2. MMP Inhibitor Screening Assay

The MMP inhibitor screening assay took place in tissue culture treated black 96-well plate (VWR). The fibronectin coated scaffolds were aspirate dried and inserted into each wells of three 96-well plates except the outer most rows. Cells were seeded into scaffold 0.8 million cells per well. DQ-gelatin was dissolved in reaction buffer and transfer to 96-well plate to have final concentration of 50 µg/mL. The concentration of BB-94 and TIMP-1 were varied from 20-1000 nM (9.55-477.64 ng/mL) and 0.1-2 µg/mL respectively. The total reaction volume in each well is 200 µL. Each condition was prepared in triplicated. The outer most rows were filled with sterile filtered deionized water and the plates were wrapped in tin foil to prevent the plates from light exposure. The 96-well plates were transferred into incubator and kept under standard tissue culture conditions 5 days. At the designate time, the emitted signal is read using plate reader set to read florescence with absorption maxima approximately at 495 nm and emission maxima approximately at 515 nm.

2.3. NIH-3T3 Viability Testing

After each time point measurement, the percent viability of NIH-3T3 for each condition was quantified by MTT (3-(4, 5-Dimethylthiazol-2-yl)-2, 5-Diphenyltetrazolium Bromide) assay following the same method as in section 2.4. NIH-3T3 viability testing from previous chapter. The estimate of viable cell number is proportional to the absorbance value at 570 nm.

2.4. Statistical Analysis

Numerical data for fluorescence signal and MTT viability assay were assessed by JMP Pro11/ statistical analysis package. Analysis of variance (ANOVA) were performed to determine statistical significant between groups, i.e. inhibitor or concentration, followed by Tukey test once significant difference were detected. Statistical significance was considered at p values of less than 0.05.

3. Result and Discussion

3.1. MMP Screening Assay

Following incubation of 50 µg/mL DQ-gelatin with NIH-3T3 in presence of either TIMP-1 or BB-94 at different concentrations under standard tissue culture condition (5% CO_2, 95% humidity at 37°C) for 5 days, the emitted fluorescence was measured. TIMP-1 was tested at 0.1, 0.375, 0.75 and 2 µg/mL and BB-94 at 20, 250, 750 and 1000 nM. The ranges of MMP inhibitor concentration were selected based on their potency under physiological conditions to elicit the ability of our prototype in MMP inhibition detection not for efficacy comparison. Statistical analysis suggests that the signal generated in consequence of culturing cells in presence of DQ-gelatin is significantly different from the background fluorescence ($n=3$, $p<0.05$), detail discussion mentioned in prototype development.

From the 96-well plate used as experiment vessel, fluorescence emission from well containing MMP inhibitor was compared to wells without inhibitors to visualize the enzyme inhibition potency as the level of fluorescence correlated with the extent of DQ-gelatin break down. The concentration of each inhibitor was varied, each condition were prepared in triplicates. The data obtained is present as bar chart in the form of percentage of the DQ-gelatin degradation without the inhibitory effect of MMP inhibitor (Figure 16). TIMP-1 demonstrated maximum inhibition potency of 60.00±27.41 % at the concentration of 2 µg/mL and BB-94 displayed maximum inhibition potency of 72.59±4.75 % at the concentration of 1000 nM.

The initial assessment using Analysis of variance (ANOVA) considering each distinct condition, type of inhibitor and concentration of inhibitor as one treatment shows significant difference between different treatment ($p<0.05$), (Figure 17a). To determine which pairS of treatments are statistically different another ANOVA and Tukey test were performed. The analysis suggests that there is significant difference between the inhibitory effect of TIMP-1 and BB-94 (Figure 17b) but variation in their concentration does not influence the inhibitor efficacy in a significant level (Figure 17c). To conclude the overall efficacy of both MMP inhibitors over the chosen concentration range, TIMP-1 post 43.80±18.62% inhibitory effect while BB-94 shows 63.67±7.5% degradation inhibition over the experimental period of 5 days.

To compare inhibition efficacy of BB-94 and TIMP-1, BB-94 possesses higher inhibition potency with smaller standard deviation. Because there are no detectable statistical difference in the inhibitory effect of BB-94 the best concentration would be the lowest concentration, 20 nM. Despite TIMP-1 does not have detectable significant difference between each concentration, T3 has no significant inhibitory effect, thus, it is best to select the concentration report to be most potent, 2 µg/mL. As there is no statistical difference in the efficacy of these 2 conditions, it could be roughly concluded that BB-94 is approximately 200 times more potent than TIMP-1 at concentration 20 nM or approximately 9.55 ng/mL.

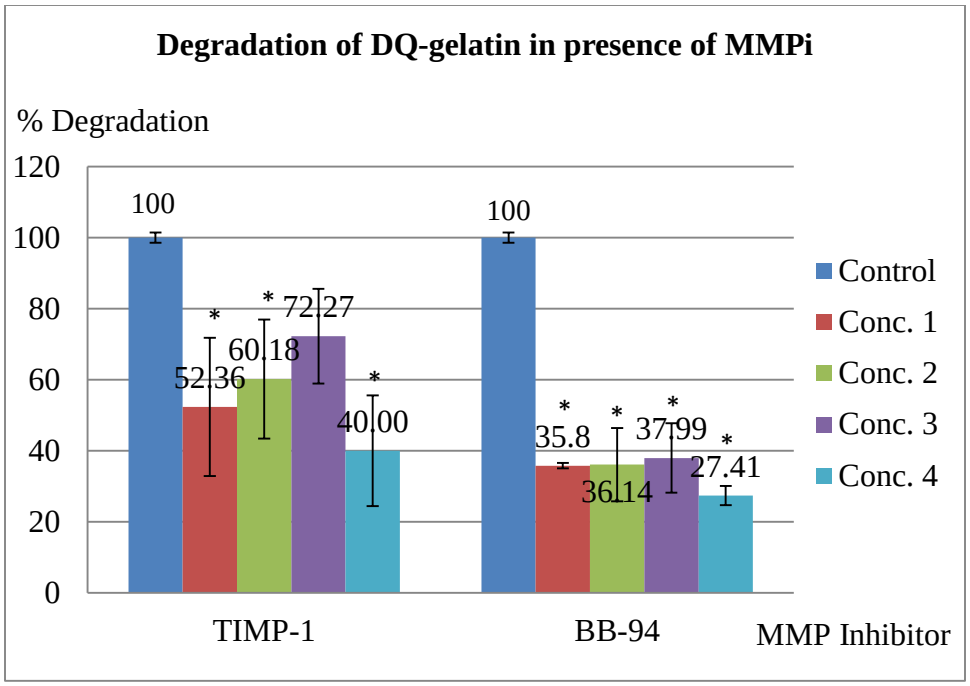

Figure 16a Degradation of DQ-gelatin and MMP inhibitor efficacy measurement. Degradation of DQ-gelatin in presence of MMP inhibitor. Timp-1 and BB-94 were tested at concentration 0.1, 0.375, 0.75 and 2 µg/mL and 20, 250, 750 and 1000 nM respectively.

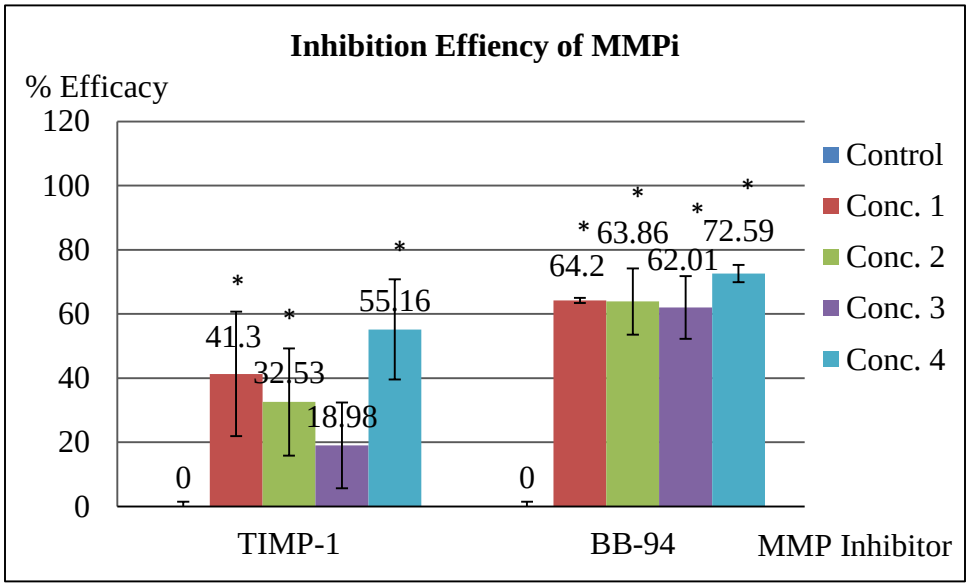

Figure 16b Degradation of DQ-gelatin and MMP inhibitor efficacy measurement. Inhibition efficacy of MMP inhibitor, the reduction from 100 percent degradation indicates the inhibitory effect of TIMP-1 and BB-94. Values are mean ± SD; (n=3, *p≤0.05 vs. control)

Analysis of Variance				
Source	DF	Sum of Squares	Mean Square	F Ratio
Model	8	12710.892	1588.86	8.2630
Error	18	3461.137	192.29	Prob > F
C. Total	26	16172.029		0.0001*

Figure 17a Statistical analysis. ANOVA of MMP inhibitor screening assay result; treating each concentration of each inhibitor as one treatment (n=3, $p<0.05$)

Analysis of Variance				
Source	DF	Sum of Squares	Mean Square	F Ratio
Model	2	10857.054	5428.53	24.5128
Error	24	5314.975	221.46	Prob > F
C. Total	26	16172.029		<.0001*

Figure 17b Statistical analysis. b) ANOVA of MMP inhibitor screening assay result; treating each type of inhibitor as one treatment (n=12, $p<0.05$)

Level				Least Sq Mean
cntrl	A			100.00000
T3	A	B		72.27139
T2		B	C	60.18167
T1		B	C	52.35754
T4		B	C	40.00094
B3		B	C	37.98755
B2		B	C	36.13803
B1		B	C	35.80091
B4			C	27.41490

Figure 17 Statistical analysis. Tukey test on cell viability of different conditions, levels not connected by same letter are significantly different.

3.2.NIH-3T3 Viability Testing

Analysis of Variance				
Source	DF	Sum of Squares	Mean Square	F Ratio
Model	8	14356.023	1794.50	0.9203
Error	18	35099.247	1949.96	Prob > F
C. Total	26	49455.271		0.5226

Figure 18 Analysis of variance on cell viability after MMP inhibitor screening assay. ANOVA of NIH-3T3 viability; treating each specific condition; each type of inhibitor and the concentration as treatment (n=3, $p<0.05$)

After MMP inhibitor screening assay was complete, fluorescence measurement taken, MTT viability assay was performed to ensure cells remain alive throughout 5-day incubation period. MTT solution was insert into each experimental compartment, mitochondrial dehydrogenase in viable cells would convert yellow MTT into purple formazan crystal which could be detected by measuring absorbance at 570 nm after solubilization. Analysis of variance shows no significant difference between each conditions (n=3, p=0.05), Figure 18 over 5 days, NIH-3T3 in each condition had proliferated to 238±35.17% the original seeded cell number. These results suggest that our assay gave satisfactory performance in maintaining cell viability throughout the experiment period.

4. Conclusion

The purpose of Cell-based MMP inhibitor screening assay experiments is to observe whether our developed assay could display the inhibitory potential of our selected MMP inhibitors as we have postulated. We hypothesized that the introduction of MMP inhibitor would reduce the proteolytic activity within the experimental volume, which could be determined by the reduction of emitted fluorescence caused by DQ-gelatin breakdown. Experiment were carried out using the optimized conditions obtained from novel assay development process, 0.8 million cells seeded on scaffold incubated for 5 days in presence of 50 µg/mL of DQ-gelatin, together with varied concentrations of MMP inhibitors; 0.1-2 µg/mL and 20-1000 nM for Timp-1 and BB-94. The outcomes were of satisfactory that each experiment containing MMP inhibitor shows reduction in fluorescence signal when compare to the control group that has no MMP inhibitor within the experiment. TIMP-1 exhibit maximum inhibition potency of 60.00±27.41 % at the concentration of 2 µg/mL and BB-94 72.59±4.75 % at the concentration of 1000 nM after 5 days incubation. From these results, we conclude that our constructed novel cell-based assay could be used to determine the efficacy in impeding proteolytic activity and thus be utilized as a tool for MMP inhibitor screening.

CHAPTER 5: CONCLUSION AND RECOMMENDATION FOR FUTURE RESEARCH

We believe that based on fluorescence emission emitted from DQ-gelatin we could estimate the inhibitory efficacy of MMPi in protein proteolysis and use this concept to construct MMP inhibitor screening assay. From assay prototype development, it has been demonstrated that cell driven breakdown of DQ-gelatin created a reliable fluorescent signal that is statistically different from the background noise. The most favorable condition for signal optimization that can maintain NIH-3T3 viability defined during the development is used as the setting for MMP inhibitor screening assay.

The efficacy BB-94 and TIMP-1, our MMP inhibitor of choice were examined. The concentration range of these inhibitor were based on the estimate value of MMP in tissue and their half maximal inhibitory concentration value; Timp-1 0.1-2 µg/mL and BB-94 20-1000 nM or 9.55-477.64 ng/mL. After 5 days incubation of 0.8 million NIH-3T3 cells in presence of 50 µg/mL DQ-gelatin with varying amount of MMP inhibitor, the fluorescence signal is measured. The signal was translated into the percentage of the fluorescence signal emitted by the control where no inhibitor was added and the decrease in the value is reported as the inhibitor efficacy of the inhibitor.

From our assay, TIMP-1 exhibit maximum inhibition potency of 60.00±27.41 % at the concentration of 2 µg/mL and BB-94 72.59±4.75 % at the concentration of 1000 nM. The statistical analysis showed no significant difference between each concentration of inhibitors. Therefore, to conclude our result, the overall inhibitory efficacy of MMP inhibitors over the

chosen concentration range for TIMP-1 is 43.80±18.62% and BB-94 is 63.67±7.5% over the experimental period of 5 days. BB-94 proves to be the more attractive potential MMP inhibitor for implant lifetime prolongation with its higher inhibitory efficacy, less in result variations and relatively lower cost.

By being capable of displaying optimal concentration and efficacy of MMPi while maintaining cell viability we believe our novel cell-based assay is a feasible assay for inhibitor screening that represents the complex degradation process of protein based implant in biological system better than the current conventional enzyme-based methods. Because of the high cost of MMPs, our assay may serve as a less costly alternative and would shorten the process of cytotoxicity test if the chosen MMP inhibitor would later be tested in the in vivo experiment.

For future directions, the improvements of the novel assay could be conducted by simplifying cell adhesion support scaffold fabrication process by changing types of materials and optimizing their capacity to support viability of high cell number. In this way, the assay would gain more practicality and would be more easy to use.

Other than the capability of the assay, from this research, we may be able to conclude that MMP inhibitors may be used to impede protein degradation process, thus, is a potential substance that could be used to be co-delivered with protein based material to extend the implant retention time in vivo. Further researches are required to before this scheme may successfully take place. As MMP are crucial for ECM remodeling process which is a natural mechanism which should go

uninterrupted, introducing MMP without retaining them to the implant cite may bring about negative side effects. Furthermore because MMP modulated proteolytic degradation is confined to a close space near cell periphery [56], MMPi efficacy would detrimentally decrease if let dispersed to surrounding area. For this reason, introduction of MMP inhibitor may be a feasible means of extending lifetime of protein based implants but there is still considerable distance before their actual usage. A proper conjugation method to couple MMP inhibitor to the implants may be the crucial next step towards the particular improvements in therapeutic efficacy.

CHAPTER 6: REFERENCES

[1] Klein, A. W. (2001). Skin filling. Collagen and other injectables of the skin. Dermatologic Clinics, 19(3), 491.

[2] Badylak, S., Kropp, B., McPherson, T., Liang, H., & Snyder, P. (1998). Small intestinal submucosa: A rapidly resorbed bioscaffold for augmentation cystoplasty in a dog model. Tissue Engineering, 4(4), 379-387.

[3] Rickey, F. A., Elmore, D., Hillegonds, D., Badylak, S., Record, R., & Simmons-Byrd, A. (2000). Re-generation of tissue about an animal-based scaffold: AMS studies of the fate of the scaffold. Nuclear Instruments and Methods in Physics Research Section B: Beam Interactions with Materials and Atoms, 172(1), 904-909.

[4] Klein, A. W. (1988). Indications and implantation techniques for the various formulations of injectable collagen. The Journal of Dermatologic Surgery and Oncology, 14(s1), 27-30.

[5] Schense, J. C., Bloch, J., Aebischer, P., & Hubbell, J. A. (2000). Enzymatic incorporation of bioactive peptides into fibrin matrices enhances neurite extension. Nature Biotechnology, 18(4), 415-419.

[6] Shin, H., Jo, S., & Mikos, A.G. (2003). Biomimetic materials for tissue engineering. Biomaterials, 24(24), 4353-4364.

[7] Singelyn, J. M., DeQuach, J. A., Seif-Naraghi, S. B., Littlefield, R. B., Schup-Magoffin, P. J., & Christman, K. L. (2009). Naturally derived myocardial matrix as an injectable scaffold for cardiac tissue engineering. Biomaterials, 30(29), 5409-5416.

[8] Stock, U. A., & Vacanti, J. P. (2001). Tissue engineering: Current state and prospects. Annual Review of Medicine, 52(1), 443-451.

[9] Wang, H., Li, Y., Zuo, Y., Li, J., Ma, S., & Cheng, L. (2007). Biocompatibility and osteogenesis of biomimetic nano-hydroxyapatite/polyamide composite scaffolds for bone tissue engineering. Biomaterials, 28(22), 3338-3348.

[10] Yang, S., Leong, K., Du, Z., & Chua, C. (2002). The design of scaffolds for use in tissue engineering. Part II. Rapid prototyping techniques. Tissue Engineering, 8(1), 1-11.

[11] Shortliffe, L. M., Freiha, F. S., Kessler, R., Stamey, T. A., & Constantinou, C. E. (1989). Treatment of urinary incontinence by the periurethral implantation of glutaraldehyde cross-linked collagen. The Journal of Urology, 141(3), 538-541.

[12] Bailey, A. J. (2000). The fate of collagen implants in tissue defects. Wound Repair and Regeneration, 8(1), 5-12.

[13] Parks, W. C. (1999). Matrix metalloproteinases in repair. Wound Repair and Regeneration, 7(6), 423-432.

[14] Kähäri, V., & Saarialho-Kere, U. (1999). Trendsin molecular medicine: Matrix metalloproteinases and their inhibitors in tumour growth and invasion. Annals of Medicine, 31(1), 34-45.

[15] Nagase, H., & Woessner, J. F., Jr. (1999). Matrix metalloproteinases. The Journal of Biological Chemistry, 274(31), 21491-21494.

[16] Gomez, D. E., Alonso, D. F., Yoshiji, H., & Thorgeirsson, U. P. (1997). Tissue inhibitors of metalloproteinases: Structure, regulation and biological functions. European Journal of Cell Biology, 74(2), 111-122.

[17] Kleiner, D. E., & Stetlerstevenson, W. G. (1994). Quantitative zymography: Detection of picogram quantities of gelatinases. Analytical Biochemistry, 218(2), 325-329.

[18] Woessner, J. F.,Jr. (1995). Quantification of matrix metalloproteinases in tissue samples. Methods in Enzymology, 248, 510-528.

[19] Leber, T. M., & Balkwill, F. R. (1997). Zymography: A single-step staining method for quantitation of proteolytic activity on substrate gels. Analytical Biochemistry, 249(1), 24-28.

[20] Drury, J. L., & Mooney, D. J. (2003). Hydrogels for tissue engineering: Scaffold design variables and applications. Biomaterials, 24(24), 4337-4351.

[21] Hutmacher, D.W. (2002). Scaffolds in tissue engineering bone and cartilage. Biomaterials, 21(24), 2529-2543.

[22] Lakhani, R., Fishman, J. M., Bleach, N., & Costello, D. (2011). Injectable materials for vocal fold medialisation in unilateral vocal fold paralysis. The Cochrane Library, *354* (supl I):32-4

[23] Mallur, P. S., & Rosen, C. A. (2010). Vocal fold injection: Review of indications, techniques, and materials for augmentation. Clinical and Experimental Otorhinolaryngology, 3(4), 177-182.

[24] E, Lexer. (1911). Euber freie fettransplantation. Klin Ther Wehnschr, 18, 53.

[25] Ersek, R. A. (1991). Transplantation of purified autologous fat: A 3-year follow-up is disappointing. Plastic and Reconstructive Surgery, 87(2), 219-227.

[26] Gray, S. D. (2000). Cellular physiology of the vocal folds. Otolaryngologic Clinics of North America, 33(4), 679-697.

[27] Duflo, S., Thibeault, S. L., Li, W., Shu, X. Z., & Prestwich, G. D. (2006). Vocal fold tissue repair in vivo using a synthetic extracellular matrix. Tissue Engineering, 12(8), 2171-2180.

[28] Gray, S. D., Titze, I. R., Alipour, F., & Hammond, T. H. (2000). Biomechanical and histologic observations of vocal fold fibrous proteins. The Annals of Otology, Rhinology, and Laryngology, 109(1), 77-85.

[29] Chan, R. W., & Titze, I. R. (2000). Viscoelastic shear properties of human vocal fold mucosa: Theoretical characterization based on constitutive modeling. The Journal of the Acoustical Society of America, 107(1), 565-580.

[30] Titze, I. R. (1992). Phonation threshold pressure: A missing link in glottal aerodynamics. The Journal of the Acoustical Society of America, 91(5), 2926-2935.

[31] Titze, I. R. (1988). The physics of small-amplitude oscillation of the vocal folds. The Journal of the Acoustical Society of America, 83(4), 1536-1552.

[32] Duranti, F., Salti, G., Bovani, B., Calandra, M., & Rosati, M. L. (1998). Injectable hyaluronic acid gel for soft tissue augmentation. Dermatologic Surgery, 24(12), 1317-1325.

[33] Thibeault, S. L., Klemuk, S. A., Chen, X., & Quinchia Johnson, B. H. (2011). < i> in Vivo</i> engineering of the vocal fold ECM with injectable HA Hydrogels—Late effects on tissue repair and biomechanics in a rabbit model. Journal of Voice, 25(2), 249-253.

[34] Cohen, J. L., Dayan, S. H., Brandt, F. S., Nelson, D. B., Axford-Gatley, R. A., Theisen, M. J., & Narins, R. S. (2013). Systematic review of clinical trials of Small-and Large-Gel-Particle hyaluronic acid injectable fillers for aesthetic soft tissue augmentation. Dermatologic Surgery, 39(2), 205-231.

[35] D, P. (1994). Crosslinked hyaluronic acid (hylan gel) as a soft tissue augmentation material: A preliminary assessment. Elson, ML (Ed): Evaluation and Treatment of the Aging Face. New York, Springer, 304-308.

[36] Necas, J., Bartosikova, L., Brauner, P., & Kolar, J. (2008). Hyaluronic acid (hyaluronan): A review. Veterinarni Medicina, 53(8), 397-411.

[37] Hallén, L., Dahlqvist, Å., & Laurent, C. (1998). Dextranomeres in hyaluronan (DiHA): A promising substance in treating vocal cord insufficiency. The Laryngoscope, 108(3), 393-397.

[38] Nelson, C. M., & Tien, J. (2006). Microstructured extracellular matrices in tissue engineering and development. Current Opinion in Biotechnology, 17(5), 518-523.

[39] Badylak, S. F. (2007). The extracellular matrix as a biologic scaffold material. Biomaterials, 28(25), 3587-3593.

[40] Badylak, S. F., Freytes, D. O., & Gilbert, T. W. (2009). Extracellular matrix as a biological scaffold material: Structure and function. Acta Biomaterialia, 5(1), 1-13.

[41] Badylak, S. F. (2002). The extracellular matrix as a scaffold for tissue reconstruction. Seminars in Cell & Developmental Biology, 13(5) 377-383.

[42] Schultz, G. S., Ladwig, G., & Wysocki, A. (2005). Extracellular matrix: Review of its roles in acute and chronic wounds. World Wide Wounds, 2005.

[43] Chen, X., & Thibeault, S. L. (2010). Biocompatibility of a synthetic extracellular matrix on immortalized vocal fold fibroblasts in 3-D culture. Acta Biomaterialia, 6(8), 2940-2948.
[44] Shu, X. Z., Ahmad, S., Liu, Y., & Prestwich, G. D. (2006). Synthesis and evaluation of injectable, in situ crosslinkable synthetic extracellular matrices for tissue engineering. Journal of Biomedical Materials Research Part A, 79(4), 902-912.

[45] Di Lullo, G. A., Sweeney, S. M., Korkko, J., Ala-Kokko, L., & San Antonio, J. D. (2002). Mapping the ligand-binding sites and disease-associated mutations on the most abundant protein in the human, type I collagen. The Journal of Biological Chemistry, 277(6), 4223-4231.

[46] Karsenty, G., & Park, R. (1995). Regulation of type I collagen genes expression. International Reviews of Immunology, 12(2-4), 177-185.

[47] Boateng, J. S., Matthews, K. H., Stevens, H. N., & Eccleston, G. M. (2008). Wound healing dressings and drug delivery systems: A review. Journal of Pharmaceutical Sciences, 97(8), 2892-2923.

[48] Sai K, P., & Babu, M. (2000). Collagen based dressings—a review. Burns, 26(1), 54-62.

[49] Knapp, T. R., Kaplan, E. N., & Daniels, J. R. (1977). Injectable collagen for soft tissue augmentation. Plastic and Reconstructive Surgery, 60(3), 398-405.

[50] Baumann, L., Kaufman, J., & Saghari, S. (2006). Collagen fillers. Dermatologic Therapy, 19(3), 134-140.

[51] Cheng, J. T., Perkins, S. W., & Hamilton, M. M. (2002). Collagen and injectable fillers. Otolaryngologic Clinics of North America, 35(1), 73-85.

[52] Baumann, L. (2006). Collagen-containing fillers: Alone and in combination. Clinics in Plastic Surgery, 33(4), 587-596.

[53] Cheung, H., Lau, K., Lu, T., & Hui, D. (2007). A critical review on polymer-based bio-engineered materials for scaffold development. Composites Part B: Engineering, 38(3), 291-300.

[54] Syrett, B., & Acharya, A. (1979). Corrosion and degradation of implant materials ASTM International.

[55] Azevedo, H. S., Gama, F. M., & Reis, R. L. (2003). In vitro assessment of the enzymatic degradation of several starch based biomaterials. Biomacromolecules, 4(6), 1703-1712.

[56] Werb,Z. (1997). ECM and cell surface proteolysis: Regulating cellular ecology. *Cell, 91*(4), 439-442. Bailey,A.J. (2000).

[57] Rothe, M., & Falanga, V. (1989). Growth factors their biology and promise in dermatologic diseases and tissue repair. Archives of Dermatology, 125(10), 1390-1398.

[58] Shakespeare, P. (2001). Burn wound healing and skin substitutes. Burns, 27(5), 517-522.

[59] Bennett, N. T., & Schultz, G. S. (1993). Growth factors and wound healing: Part II. Role in normal and chronic wound healing. The American Journal of Surgery, 166(1), 74-81.

[60] Bennett, N. T., & Schultz, G. S. (1993). Growth factors and wound healing: Biochemical properties of growth factors and their receptors. The American Journal of Surgery, 165(6), 728-737.

[61] Lawrence, W. T. (1998). Physiology of the acute wound. Clinics in Plastic Surgery, 25(3), 321-340.

[62] Diegelmann, R.F., & Evans, M.C. (2004). Wound healing: An overview of acute, fibrotic and delayed healing. Front Biosci, 9(1), 283-289.

[63] Martin, P. (1997). Wound healing--aiming for perfect skin regeneration. Science (New York, N.Y.), 276(5309), 75-81.

[64] Greiling, D., & Clark, R. A. (1997). Fibronectin provides a conduit for fibroblast transmigration from collagenous stroma into fibrin clot provisional matrix. Journal of Cell Science, 110 (Pt 7) (Pt 7), 861-870.

[65] Eckes, B., Aumailley, M., & Krieg, T. (1988). Collagens and the reestablishment of dermal integrity. The molecular and cellular biology of wound repair (pp. 493-512) Springer.

[66] Levenson, S. M., Geever, E. F., Crowley, L. V., Oates, J. F.,3rd, Berard, C. W., &Rosen, H. (1965). The healing of rat skin wounds. Annals of Surgery, 161, 293-308.

[67] Ottesen, M. (1967). Induction of biological activity by limited proteolysis. Annual Review of Biochemistry, 36(1), 55-76.

[68] Falanga, V. (2002). Wound bed preparation and the role of enzymes: A case for multiple actions of therapeutic agents. WOUNDS: A Compendium of Clinical Research and Practice, 14(2), 47-57.

[69] Alberts, B., Bray, D., Lewis, J., Raff, M., Roberts, K., & Watson, J. (1994). Molecular biology of the cell. New York: Garland Publishing, Inc., 3rd ed.

[70] Lee, C. H., Singla, A., & Lee, Y. (2001). Biomedical applications of collagen. International Journal of Pharmaceutics, 221(1), 1-22.

[71] Vaalamo, M. (2000). Matrix metalloproteinases and their inhibitors in normal and aberrant wound repair. A Dissertation.Medical Faculty, University of Helsinki.

[72] Pilcher, B. K., Dumin, J. A., Sudbeck, B. D., Krane, S. M., Welgus, H. G., & Parks, W. C. (1997). The activity of collagenase-1 is required for keratinocyte migration on a type I collagen matrix. The Journal of Cell Biology, 137(6), 1445-1457.

[73] Frederiks, W. M., & Mook, O. R. (2004). Metabolic mapping of proteinase activity with emphasis on in situ zymography of gelatinases: Review and protocols. The Journal of Histochemistry and Cytochemistry: Official Journal of the Histochemistry Society, 52(6), 711-722.

[74] Pei, D., & Weiss, S. J. (1995). Furin-dependent intracellular activation of the human stromelysin-3 zymogen,

[75] Sato, H., Kinoshita, T., Takino, T., Nakayama, K., & Seiki, M. (1996). Activation of a recombinant membrane type 1-matrix metalloproteinase (MT1-MMP) by furin and its interaction with tissue inhibitor of metalloproteinases (TIMP)-2. FEBS Letters, 393(1), 101-104.

[76] Heussen, C., & Dowdle, E. B. (1980). Electrophoretic analysis of plasminogen activators in polyacrylamide gels containing sodium dodecyl sulfate and copolymerized substrates. Analytical Biochemistry, 102(1), 196-202.

[77] Kundapur, R. R. (2013). Zymography: Enzymes in action. Science International, 1(4), 70-75.

[78] Hibbs, M. S., Hasty, K. A., Seyer, J. M., Kang, A. H., & Mainardi, C. L. (1985). Biochemical and immunological characterization of the secreted forms of human neutrophil gelatinase. The Journal of Biological Chemistry, 260(4), 2493-2500.

[79] Masure, S., Proost, P., Damme, J., & Opdenakker, G. (1991). Purification and identification of 91-kDa neutrophil gelatinase. European Journal of Biochemistry, 198(2), 391-398.

[80] Liabakk, N. B., Talbot, I., Smith, R. A., Wilkinson, K., & Balkwill, F. (1996). Matrix metalloprotease 2 (MMP-2) and matrix metalloprotease 9 (MMP-9) type IV collagenases in colorectal cancer. Cancer Research, 56(1), 190-196.

[81] Curino, A., Patel, V., Nielsen, B. S., Iskander, A. J., Ensley, J. F., Yoo, G. H., Holsinger, F. C., Mayers, J.N., El-Nagaar, A., Kellman, R. M. (2004). Detection of plasminogen activators in oral cancer by laser capture microdissection combined with zymography. Oral Oncology, 40(10), 1026-1032.

[82] Margulies, I. M., Hoyhtya, M., Evans, C., Stracke, M. L., Liotta, L. A., & Stetler-Stevenson, W. G. (1992). Urinary type IV collagenase: Elevated levels are associated with bladder transitional cell carcinoma. Cancer Epidemiology, Biomarkers &Prevention: A Publication of the American Association for Cancer Research, Cosponsored by the American Society of Preventive Oncology, 1(6), 467-474.

[83] Li, L., Chen, P., Ling, Y., Song, X., Lu, Z., He, Q., Li, Z.,Lu, Na., Guo, Q. (2011). Inhibitory effects of GL-V9 on the invasion of human breast carcinoma cells by downregulating the expression and activity of matrix metalloproteinase-2/9. European Journal of Pharmaceutical Sciences, 43(5), 393-399.

[84] Paemen, L., Olsson, T., Söderström, M., Damme, J., & Opdenakker, G. (1994). Evaluation of gelatinases and IL-6 in the cerebrospinal fluid of patients with optic neuritis, multiple sclerosis and other inflammatory neurological diseases. European Journal of Neurology, 1(1), 55-63.

[85] Paemen, L., Martens, E., Norga, K., Masure, S., Roets, E., Hoogmartens, J., & Opdenakker, G. (1996). The gelatinase inhibitory activity of tetracyclines and chemically modified tetracycline analogues as measured by a novel microtiter assay for inhibitors. Biochemical Pharmacology, 52(1), 105-111.

[86] Van den Steen, Philippe E, Dubois, B., Nelissen, I., Rudd, P. M., Dwek, R. A., & Opdenakker, G. (2002). Biochemistry and molecular biology of gelatinase B or matrix metalloproteinase-9 (MMP-9). Critical Reviews in Biochemistry and Molecular Biology, 37(6), 375-536.

[87] Vandooren, J., Geurts, N., Martens, E., Van den Steen, Philippe E, & Opdenakker, G. (2013). Zymography methods for visualizing hydrolytic enzymes. Nature Methods, 10(3), 211-220.

[88] Wilkesman, J., & Kurz, L. (2009). Protease analysis by zymography: A review on techniques and patents. Recent Patents on Biotechnology, 3(3), 175-184.

[89] Duran-Vilaregut, J., Del Valle, J., Manich, G., Camins, A., Pallàs, M., Vilaplana, J., & Pelegrí, C. (2011). Role of matrix metalloproteinase-9 (MMP-9) in striatal blood–brain barrier disruption in a 3-nitropropionic acid model of huntington's disease. Neuropathology and Applied Neurobiology, 37(5), 525-537.

[90] Brinckerhoff, C. E., & Matrisian, L. M. (2002). Matrix metalloproteinases: A tail of a frog that became a prince. Nature Reviews Molecular Cell Biology, 3(3), 207-214.

[91] Neuruth, H. (1957). The activation of zymogens. Adv.Protein Chem, 12, 319.

[92] Clark,I.M., Swingler, T.E., Sampieri, C.L., & Edwards,D.R. (2008). The regulation of matrix metalloprotienases and their inhibitors, The International Journal of Biochemistry & cell Biology, 40(6), 1362-1378.

[93] Masure, S., Billiau, A., Van Damme, J., & Opdenakker, G. (1990). Human hepatoma cells produce an 85 kDa gelatinase regulated by phorbol 12-myristate 13-acetate. Biochimica Et Biophysica Acta (BBA)-Molecular Cell Research, 1054(3), 317-325.

[94] Kleiner, D. E., & Stetlerstevenson, W. G. (1994). Quantitative zymography: Detection of picogram quantities of gelatinases. Analytical Biochemistry, 218(2), 325-329.

[95] Ikeda, M., Maekawa, R., Tanaka, H., Matsumoto, M., Takeda, Y., Tamura, Y., Nemori, R., Yoshioka, T. (2000). Inhibition of gelatinolytic activity in tumor tissues by synthetic matrix metalloproteinase inhibitor: Application of film in situ zymography. Clinical Cancer Research: An Official Journal of the American Association for Cancer Research, 6(8), 3290-3296.

[96] Fluorescence. (2014). In Encyclopaedia Britannica. Retrieved from http://www.britannica.com/EBchecked/topic/211338/fluorescence.

[97]Oh, L. Y., Larsen, P. H., Krekoski, C. A., Edwards, D. R., Donovan, F., Werb, Z., & Yong, V. W. (1999). Matrix metalloproteinase-9/gelatinase B is required for process outgrowth by oligodendrocytes. The Journal of Neuroscience: The Official Journal of the Society for Neuroscience, 19(19), 8464-8475.

[98] Lee, S. R., Tsuji, K., Lee, S. R., & Lo, E. H. (2004). Role of matrix metalloproteinases in delayed neuronal damage after transient global cerebral ischemia. The Journal of Neuroscience: The Official Journal of the Society for Neuroscience, 24(3), 671-678.

[99] Desmoulière, A., & Gabbiani, G. (1988). The role of the myofibroblast in wound healing and fibrocontractive diseases. The molecular and cellular biology of wound repair (pp. 391-423) Springer.

[100] Tarnuzzer, R. W., & Schultz, G. S. (1996). Biochemical analysis of acute and chronic wound environments. Wound Repair and Regeneration, 4(3), 321-325.

[101] Cawston, T. E., & Wilson, A. J. (2006). Understanding the role of tissue degrading enzymes and their inhibitors in development and disease. Best Practice & Research Clinical Rheumatology, 20(5), 983-1002.

[102] Nagase, H., Visse, R., & Murphy, G. (2006). Structure and function of matrix metalloproteinases and TIMPs. Cardiovascular Research, 69(3), 562-573.

[103] Todaro, G. J., & Green, H. (1963). Quantitative studies of the growth of mouse embryo cells in culture and their development into established lines. The Journal of Cell Biology, 17, 299-313.

[104] Ravanti, L., & Kähäri, V. (2000). Matrix metalloproteinases in wound repair (review). International Journal of Molecular Medicine, 6(4), 391-798.

[105] Chiarugi, P., & Giannoni, E. (2008). < i> Anoikis</i>: A necessary death program for anchorage-dependent cells. Biochemical Pharmacology, 76(11), 1352-1364.

[106] Walker, A. M. (2014) Optimization in vitro extracellular matrix production using polymer scaffolds with targeted pore size. (Unpublished thesis). University of Arkansas, Fayetteville.

[107] Salo, T., Makela, M., Kylmaniemi, M., Autio-Harmainen, H., & Larjava, H. (1994). Expression of matrix metalloproteinase-2 and -9 during early human wound healing. Laboratory Investigation; a Journal of Technical Methods and Pathology, 70(2), 176-182.

[108] Inoue, M., Kratz, G., Haegerstrand, A., & Ståhle-Bäckdahl, M. (1995). Collagenase expression is rapidly induced in wound-edge keratinocytes after acute injury in human skin, persists during healing, and stops at re-epithelialization. Journal of Investigative Dermatology, 104(4).

[109] Ramnath, N., & Creaven, P. J. (2004). Matrix metalloproteinase inhibitors. Current Oncology Reports, 6(2), 96-102.

[110] Coussens, L. M., Fingleton, B., & Matrisian, L. M. (2002). Matrix metalloproteinase inhibitors and cancer: Trials and tribulations. Science (New York, N.Y.), 295(5564), 2387-2392.

[111] Whittaker, M., & Ayscough, A. (2001). Matrix metalloproteinases and their inhibitors—current status and future challenges. Celltransmissions, 17(1), 3-14.

[112] Zucker, S., Cao, J., & Chen, W. (2000). Critical appraisal of the use of matrix metalloproteinase inhibitors in cancer treatment. Oncogene, 19(56).

[113] Matrisian, L. M., Sledge, G. W.,Jr, & Mohla, S. (2003). Extracellular proteolysis and cancer: Meeting summary and future directions. Cancer Research, 63(19), 6105-6109.

[114] DiMartino, M., High, W., Galloway, W., & Crimmin, M. (1994). Preclinical antiarthritic activity of matrix metalloproteinase inhibitors. Annals of the New York Academy of Sciences, 732(1), 411-413.

[115] Eccles, S. A., Box, G. M., Court, W. J., Bone, E. A., Thomas, W., & Brown, P. D. (1996). Control of lymphatic and hematogenous metastasis of a rat mammary carcinoma by the matrix metalloproteinase inhibitor batimastat (BB-94). Cancer Research, 56(12), 2815-2822.

[116] Wang, X., Fu, X., Brown, P. D., Crimmin, M. J., & Hoffman, R. M. (1994). Matrix metalloproteinase inhibitor BB-94 (batimastat) inhibits human colon tumor growth and spread in a patient-like orthotopic model in nude mice. Cancer Research, 54(17), 4726-4728.

[117] Sledge, G. W.,Jr, Qulali, M., Goulet, R., Bone, E. A., & Fife, R. (1995). Effect of matrix metalloproteinase inhibitor batimastat on breast cancer regrowth and metastasis in athymic mice. Journal of the National Cancer Institute, 87(20), 1546-1550.

[118] Hann, M. M., McCullagh, K. G., & Wadsworth, H. J. (1985). Carboxyalkyl Peptide Derivatives, 1-111.

[119] Wojtowicz-Praga, S., Low, J., Marshall, J., Ness, E., Dickson, R., Barter, J., Sale, M., McCann, P., Moore, J., Cole, A. (1996). Phase I trial of a novel matrix metalloproteinase inhibitor batimastat (BB-94) in patients with advanced cancer. Investigational New Drugs, 14(2), 193-202.

[120] Pavlaki, M., & Zucker, S. (2003). Matrix metalloproteinase inhibitors (MMPIs): The beginning of phase I or the termination of phase III clinical trials. Cancer and Metastasis Reviews, 22(2-3), 177-203.

[121] Khokha, R. (1994). Suppression of the tumorigenic and metastatic abilities of murine B16-F10 melanoma cells in vivo by the overexpression of the tissue inhibitor of the metalloproteinases-1. Journal of the National Cancer Institute, 86(4), 299-304.

[122] Botos, I., Scapozza, L., Zhang, D., Liotta, L. A., & Meyer, E. F. (1996). Batimastat, a potent matrix mealloproteinase inhibitor, exhibits an unexpected mode of binding. Proceedings of the National Academy of Sciences of the United States of America, 93(7), 2749-2754.

[123] Mosmann, T. (1983). Rapid colorimetric assay for cellular growth and survival: Application to proliferation and cytotoxicity assays. Journal of Immunological Methods, 65(1), 55-63.

[124] Liu, Y., Peterson, D. A., Kimura, H., & Schubert, D. (1997). Mechanism of cellular 3-(4, 5-dimethylthiazol-2-yl)-2, 5-diphenyltetrazolium bromide (MTT) reduction. Journal of Neurochemistry, 69(2), 581-593.

[125] Berridge, M. V., & Tan, A. S. (1993). Characterization of the cellular reduction of 3-(4, 5-dimethylthiazol-2-yl)-2, 5-diphenyltetrazolium bromide (MTT): Subcellular localization, substrate dependence, and involvement of mitochondrial electron transport in MTT reduction. Archives of Biochemistry and Biophysics, 303(2), 474-482.

[126] Vistica, D. T., Skehan, P., Scudiero, D., Monks, A., Pittman, A., & Boyd, M. R. (1991). Tetrazolium-based assays for cellular viability: A critical examination of selected parameters affecting formazan production. Cancer Research, 51(10), 2515-2520.

[127] Chung, W. B., Backstrom, L. R., McDonald, J., & Collins, M. T. (1993). The (3-(4,5-dimethylthiazol-2-yl)-2,5-diphenyltetrazolium) colorimetric assay for the quantitation of actinobacillus pleuropneumoniae cytotoxin. Canadian Journal of Veterinary Research = Revue Canadienne De Recherche Veterinaire, 57(3), 159-165.

[128] Choi, J. S., Yang, H., Kim, B. S., Kim, J. D., Kim, J. Y., Yoo, B., Park, K., Lee, H. Y., Cho, Y. W. (2009). Human extracellular matrix (ECM) powders for injectable cell delivery and adipose tissue engineering. Journal of Controlled Release, 139(1), 2-7.

[129] Overall, C. M. (1994). Regulation of tissue inhibitor of matrix metalloproteinase expressiona. Annals of the New York Academy of Sciences, 732(1), 51-64.

[130] Chakraborti, S., Mandal, M., Das, S., Mandal, A., & Chakraborti, T. (2003). Regulation of matrix metalloproteinases: An overview. Molecular and Cellular Biochemistry, 253(1-2), 269-285.

[131] Steel, R., & Torrie, J. (I960). Principles and procedures of statistics with special reference to the biological sciences.